

# Beyond Algebraic Superstring Compactification: Part II

Tristan Hübsch

Department of Physics & Astronomy, Howard University, Washington, DC 20059, USA  
 thubsch@howard.edu

## ABSTRACT

The most impressively prolific exploration of superstring models (aiming for our physical reality) has been focused on worldsheet-supersymmetric gauged linear sigma models and the closely associated *complex-algebraic* toric geometry. Mirror duality relates this to the inherently *real symplectic* geometry of Calabi–Yau factors in spacetime, implying a need for a more general, heterotic framework of analysis. In turn, a closer look at possible deformations even amongst the complex-algebraic complete intersections and toric geometry models themselves indicates an a priori non-algebraic type of generalization that however perfectly aligns with requirements of mirror duality.

## Contents

<b>1</b>	<b>Introduction, Rationale and Summary</b>	<b>0</b>
1.1	Worldsheet Quantum Field Theory Models and Mirror Duality . . . . .	1
1.2	Reverse-Engineering Target Spacetime . . . . .	3
<b>2</b>	<b>Gauge-Quotient Phases of the Showcasing Sequence</b>	<b>4</b>
2.1	Field Space Gauge-Orbits . . . . .	6
2.2	VEVs and Phases . . . . .	9
<b>3</b>	<b>Deformation Family of Ambient Spaces</b>	<b>11</b>
3.1	Biprojective vs. Toric Renditions . . . . .	12
3.2	Toric Classification . . . . .	16
3.3	The Anticanonical System . . . . .	17
<b>4</b>	<b>Reflexions in the Mirror</b>	<b>24</b>
4.1	Non-Convexity and Self-Crossing . . . . .	25
4.2	The Transposed GLSM . . . . .	26
4.3	Ambient Unitary Torus Manifolds . . . . .	28
<b>5</b>	<b>Conclusions and Outlook</b>	<b>31</b>

## 1 Introduction, Rationale and Summary

Gauge anomaly detection and cancellation is a powerful tool in quantum field theory (QFT) and has 42 years ago opened the floodgates on superstring theory as a framework in which to construct models of our physical reality [1–3]. Tantamount to several anomaly cancellation conditions in the underlying worldsheet QFT of the string, Ricci-flatness of the target spacetime insures worldsheet quantum stability [4–7], as well as the self-consistency of the full, oriented loop-space reformulation [8–18]. The initially mostly analytic analysis was soon bolstered and reframed, if not entirely replaced, by algebraic methods (see [18]), especially so by the special class of worldsheet (2, 2)-supersymmetric gauged linear sigma models (GLSM) [19, 20]. Soon generalized by relaxing to (0, 2)-supersymmetry (see [21], and [22] for a more recent review), this approach has provided us with the largest pool of constructions [23, 24], well-framed within complex-algebraic and toric geometry [25–31], counted in terms of astounding “heptigoogol of moles” ( $10^{723}$ ) [18, 32]. Finding the model that matches our own World in such a mind-boggling sea of possibilities would seem like a forlorn quest, were it not for the astonishing developments in machine-learning, which more and more capably and accurately extract physical data for this quest [33–38].

The fact remains, however, that the  $(2, 2)$ - and even  $(0, 2)$ -supersymmetric GLSM framework has been chosen primarily for computational convenience: Ultimately, worldsheet  $(0, 1)$ -supergravity suffices to guarantee stable ground-states, but implies neither supersymmetry nor complex structure in the target-spacetime physics; these emerge in sectors with at least  $(0, 2)$ -supersymmetry [39–42]. In particular, its a priori *complex-algebraic* setting frames the original approach to mirror duality [43–46] (see also [47]) and dovetails with complex-algebraic toric geometry [48–50]. This framing was however neither intended nor designed to study the later discovered (real) symplectic aspects of mirror duality [51–53]; recent study indeed seems to indicate a need for generalizations [54–59]. In any case, one follows the general strategy of identifying/constructing the Ricci-flat manifolds of our ultimate interest in some *well-known* “ambient” spaces and by *well-known* methods—including the well-trodden algebraic ones.<sup>1</sup>

With this goal in mind and following [59], this article aims to: (1) revisit the physics (GLSM quantum field theory) links to toric geometry and identify avenues for generalization; (2) explore in more detail the explicitly continuous showcasing family of examples, realized as hypersurfaces in Hirzebruch scrolls,  $\mathcal{X} \in F_m^{(n)}[c_1]$ ; <sup>2</sup> (3) motivate extensions to (a priori, not complex) *unitary torus manifolds* (UTMs) [64–75] as likely candidate ambient spaces in which to find mirror-models,  $\tilde{\mathcal{X}} \in \check{F}_m^{(n)}[c_1]$ , of hypersurfaces in *non-weak-Fano*<sup>3</sup> ambient spaces,  $\mathcal{X} \in F_m^{(n)}[c_1]$ . This last aim necessarily involves (I hope) well-motivated but as yet unproven claims and conjectures, inviting more systematic and rigorous research.

The remainder of this introduction reviews the relevant key features of the worldsheet view of superstrings and how they induce the target-spacetime geometry and dynamics, focusing on the  $(2, 2)$ -supersymmetric GLSM; although widely available in the literature, it will be convenient to have these in one place for reference and reconsidering. Section 2 presents the showcasing example, where the  $U(1; \mathbb{C})^2$  gauge-symmetry acting on an array of differently-charged chiral superfields already results in an intricate field space; in a “geometric” phase, this includes generalizations of Hirzebruch (rational, ruled) surface scrolls [25, 27–30, 77, 78], and so generalizes them into the worldsheet QFT framework. Section 3 presents the explicit deformation families of Hirzebruch surfaces of arbitrarily high twist, to serve as “well-known” ambient spaces for constructing Calabi–Yau hypersurfaces. Turning to the construction of mirror models [54–59], Section 4 explores the indicated need for extending the complex-algebraic toric geometry framework and proposes a likely avenue. A brief summary of these features then motivates the outlook presented in the concluding Section 5.

### 1.1 Worldsheet Quantum Field Theory Models and Mirror Duality

Worldsheet quantum field theories are all defined on a local patch of the Riemann surface swept out by the moving string. Its dynamics in  $(2, 2)$ -supersymmetric models as considered herein<sup>4</sup> is governed by the action functional that, in its *direct* form,<sup>5</sup> includes the standard kinetic term,  $\gamma^{\alpha\beta}(\xi) (\partial_\alpha X^\mu)(\partial_\beta X^\nu) G_{\mu\nu}(X)$ ,

<sup>1</sup>This strategy has illustrious history: The very first concrete solution [60] to Einstein’s field equations made it clear that even “empty” (“sourceless,”  $T_{\mu\nu}=0$ ) observable spacetime can have a physically nontrivial geometry—and was soon aptly reconstructed by algebraic methods [61]—which makes manifest its tantalizing 2-sheeted nature and physically nontrivial global geometry [62, 63].

<sup>2</sup>In general, the symbol  $A[c_1]$  denotes the deformation family of all anticanonical (Calabi–Yau, Ricci-flat), i.e.,  $\deg_{-c_1}(A)$  hypersurfaces in the ambient space,  $A$ .

<sup>3</sup>I adopt the negation, “non-weak-Fano” [76], to mean “not even weak-Fano,” over the less precise if descriptive term, “limping” [18]: In particular,  $c_1(F_m^{(n)})$  with (“taxicab”-magnitudes)  $|\vec{m}| \geq 3$ , is positive along the fiber- $\mathbb{P}^{n-1}$ , but negative along the base- $\mathbb{P}^1$ ; in the weak-Fano case,  $|\vec{m}| = 2$ ,  $c_1(F_m^{(n)})$  vanishes along the base.

<sup>4</sup>Reducing supersymmetry,  $(2, 2) \rightarrow (0, 2)$  (or even  $\rightarrow (0, 1)$ ), may then be accomplished by expanding in, say,  $\varsigma^+$ ,  $\bar{\varsigma}^+$  (and also  $\bar{\varsigma}^-$ ), and treating the so-obtained expansion terms independently [41, 42]; see also [79–85].

<sup>5</sup>Also called the “nonlinear  $\sigma$ -model form,” this modeling is *direct* in that  $\langle X^\mu(X) \rangle$  and  $\langle G_{\mu\nu}(X) \rangle$  are local coordinates and the metric on the target-space itself—the latter of which is most of the time unknown.

for the lowest component-fields,  $X^\mu(\xi)$ , of as many chiral superfields. The vacuum expectation values (*vev*'s) of the  $X^\mu(\xi)$  serve as local coordinates (denoted by the same symbol) on the target space itself,  $\mathcal{X}$ . In turn, half of their fermionic superpartners,  $\psi_\pm^\mu$ , provide a local basis for the local tangent space, the (canonically conjugate) other half spanning the cotangent space. Here,  $\gamma^{\alpha\beta}(\xi)$  is the (inverse) metric on the worldsheet, over which the partition functional of the quantum theory is integrated. In turn,  $G_{\mu\nu}(X)$  is the target-space metric and serves as an array of coupling parameters in such worldsheet QFT models.

On a *complex* (factor of the) target spacetime,  $\mathcal{X}$ , this halving may be chosen, e.g. (see [83] and references therein),

$$G_{\mu\bar{\nu}}(X)\psi_+^{\bar{\nu}}(\xi) =: \psi_{+\mu}(\xi) \mapsto \partial_\mu \quad \text{and} \quad \psi_+^\mu(\xi) \mapsto dX^\mu, \quad (1.1a)$$

$$\text{vs.} \quad G_{\mu\bar{\nu}}(X)\psi_-^\mu(\xi) =: \psi_{-\bar{\nu}}(\xi) \mapsto \partial_{\bar{\nu}} \quad \text{and} \quad \psi_-^{\bar{\nu}}(\xi) \mapsto dX^{\bar{\nu}}. \quad (1.1b)$$

This maps the Fock-space elements to Dolbeault cohomology groups:

$$h_{\bar{\nu}_1 \dots \bar{\nu}_q}^{\mu_1 \dots \mu_p}(X, \bar{X}) \psi_-^{\bar{\nu}_1} \dots \psi_-^{\bar{\nu}_q} \psi_{+\mu_1} \dots \psi_{+\mu_p} |0\rangle \mapsto H_{\bar{0}}^q(\mathcal{X}, \wedge^p T) = H_{\bar{0}}^{n-p,q}(\mathcal{X}, \mathcal{K}^*), \quad (1.2a)$$

$$\omega_{\mu_1 \dots \mu_p \bar{\nu}_1 \dots \bar{\nu}_q}(X, \bar{X}) \psi_-^{\bar{\nu}_1} \dots \psi_-^{\bar{\nu}_q} \psi_+^{\mu_1} \dots \psi_+^{\mu_p} |0\rangle \mapsto H_{\bar{0}}^q(\mathcal{X}, \wedge^p T^*) = H_{\bar{0}}^{p,q}(\mathcal{X}), \quad (1.2b)$$

where  $\mathcal{K}_{\mathcal{X}}^* := \wedge^n T_{\mathcal{X}}$  is the anticanonical bundle of the target space,  $\mathcal{X}$ , and the rightmost equality in (1.2a) exhibits the identity  $\wedge^p T \stackrel{\text{id}}{=} \wedge^{n+(p-n)} T = \mathcal{K}^* \otimes \wedge^{n-p} T^*$ . The penultimate assignments and (1.1) make it clear that complex conjugating only the  $\psi_+ \leftrightarrow \bar{\psi}_+$  swaps  $\wedge^p T \leftrightarrow \wedge^p T^*$ , which exhibits the elementary origin of *mirror duality* in worldsheet (2, 2)-supersymmetric models:  $\tilde{\mathcal{X}}$  is the mirror of  $\mathcal{X}$  if the cohomology rings<sup>6</sup>  $H_{\bar{0}}^q(\mathcal{X}, \wedge^p T) \approx H_{\bar{0}}^q(\tilde{\mathcal{X}}, \wedge^p T^*)$ . Comparison of the ultimate, rightmost assignments in (1.2a) and in (1.2b) exhibits, in turn, that in target-spaces with a trivial (anti)canonical class,  $\mathcal{K}_{\mathcal{X}}^* = \mathcal{O}_{\mathcal{X}}$ , *mirror duality* is a symmetry of the Hodge-decomposed cohomology ring,  $H^{n-p,q}(\mathcal{X}) \approx H^{p,q}(\tilde{\mathcal{X}})$ .

The (perturbatively computed) renormalization of the worldsheet model deforms its couplings—and  $G_{\mu\nu}(X)$  in particular, which is identified as the target space metric. The requirement for stability under “quantum fluctuations” (renormalization fixed point) was found to exactly reproduce the Einstein equations in their Ricci form [4, 5],<sup>7</sup>

$$0 \stackrel{!}{=} [R_{\mu\nu} - \frac{8\pi G_N}{c^4} (T_{\mu\nu} - \frac{1}{d-2} G_{\mu\nu} G^{\rho\sigma} T_{\rho\sigma})] + O(\alpha'), \quad (1.3)$$

where  $d = \dim(\mathcal{X})$  and  $T_{\mu\nu}$  is the energy-momentum density tensor for target-spacetime “matter,” i.e., all non- $G_{\mu\nu}(X)$  degrees of freedom. Notice that the “trace-flipping” of the energy-momentum density tensor on the right-hand side of (1.3) depends on the spacetime metric,  $G_{\mu\nu}$ , and its inverse.

That the *quantum* stability of the worldsheet *quantum* field theory requires the target-spacetime metric,  $G_{\mu\nu}$ , to satisfy its *classical* equation of motion (Einstein’s field equations) may be seen as a (worldsheet-to-target spacetime) layer-building generalization of Ehrenfest’s theorem. In fact, this naturally generalizes, with *quantum* stability of more general worldsheet *quantum* field theory models inducing (with technical but not substantial  $\alpha'$ -perturbative deformations) the standard, *classical* gauge interactions in target-spacetime. Typically, it is routine to construct a target-spacetime Hamilton’s action functional from which these target-spacetime *classical* equations of motion follow via usual variational calculus. The standard Feynman path integral formalism then generates the corresponding fully fledged target-spacetime QFT model—as a candidate for the observed Standard Model physics. This “layer-cake” structure in string

<sup>6</sup>This statement of mirror duality presumes the “quantum” (deformation of the wedge) ring structure of these cohomology groups [21, 31, 51, 52]; their dimensions must agree regardless of the ring structure.

<sup>7</sup>This led to the introduction of the term “geometrostasis” [86], where Friedan’s and some earlier work was generalized, in particular also to include geometric torsion.

theory then displays the indirect nature of how string theory models our “real-world physics” as induced from a judiciously chosen underlying worldsheet model. In turn, it is also possible to focus on a “sector” within a complete model, relying on previously established connections to the rest.

Here, we focus on target-spacetimes of the form  $\mathbb{R}^{1,3} \times \mathcal{X}$ , with  $\mathbb{R}^{1,3}$  identified with the observed spacetime, and  $\mathcal{X}$  henceforth denoting a compact (and  $\leq 10^{-32}$  m small), spatial Ricci-flat factor, chosen at first so as to preserve an overall  $N = 1$  supersymmetry, which requires  $\mathcal{X}$  to be a compact, complex Calabi–Yau 3-fold; we revisit these choices in §4.

## 1.2 Reverse-Engineering Target Spacetime

Worldsheet QFT models are built over an a priori unspecified genus- $g$  Riemann surface,  $\Sigma_g$ , with a Lorentzian metric,  $\gamma_{\alpha\beta}(\xi)$ . The Feynman path integration then sums over all  $(\Sigma_g, \gamma)$ -choices as prescribed by the Deligne–Mumford “universal curve,” over specific boundary (periodic/anti-periodic, etc.) conditions, and also allows the inclusion of worldsheet boundary “sources.”

Aiming to dynamically determine the Calabi–Yau space,  $\mathcal{X}$ , one must start *somewhere*, and so one starts with a well-understood, well-known and computationally convenient *ambient space*,<sup>8</sup>  $A$ , to provide an auxiliary scaffolding within which to construct  $\mathcal{X}$  of our ultimate interest. In this sense, and in contradistinction to the discussion in §1.1, these are *indirect* constructions of Calabi–Yau spaces, via intermediate but convenient ambient spaces. GLSMs [19, 20] provide one such large class of  $(2, 2)$ -supersymmetric worldsheet models, the low-energy limit of which (in simple cases) corresponds 1–1 to nonlinear, constrained complex projective-space models [41, 42, 87–89] (and references therein), and so provide their vast generalization; see also [90]. GLSMs are well specified by providing:

1. A list of  $n+r$  chiral  $(2, 2)$ -superfields,  $X_i(\xi)$ , the lowest (bosonic) component fields of which provide (complex) coordinate fields for the (complex  $n$ -dimensional) compact factor in the target spacetime.
2. A list of  $r$  twisted-chiral  $(2, 2)$ -superfields,  $\sigma_a$ , one for each gauged  $U(1)$  symmetry. (1+1-dimensional gauge 2-vector potentials have no propagating degrees of freedom, but induce gauge-equivalences, and are accompanied by a complex scalar field each.)
3. The worldsheet  $(2, 2)$ -supersymmetric  $U(1)^r$  gauge symmetry is automatically complexified,  $U(1)^r \rightarrow U(1; \mathbb{C})^r = (\mathbb{C}^*)^r$ , and acts by nonzero complex rescaling,  $X_i \rightarrow \lambda \cdot X_i := \prod_a \lambda_a^{q_{ai}} X_i$ , where  $q_{ai} = q_a(X_i)$  is the charge of  $X_i$  with respect to the  $a^{\text{th}}$   $U(1)$ , and  $\lambda_a \in \mathbb{C}^*$  are nonzero complex-valued chiral superfields.

The Lagrangian super-density consists of the standard,  $U(1)^r$  gauge-invariant kinetic term (with the standard coupling the chiral and twisted-chiral superfields) and a superpotential for  $X$ -exclusive (“Yukawa”) interactions:

4. A choice of the superpotential, of the general form  $W(X) = \sum_{\alpha=1}^K X_0^\alpha f_\alpha(X)$ , where we focus on the  $K = 1$  (single hypersurface) case, and omit the index  $\alpha$ . The function  $f(X)$  is chosen quasi-homogeneous,  $f(\lambda \cdot X) = \prod_a \lambda^{q_{af}} f(X)$ , and  $q_a(X_0) = q_{a0}$ , so that the superpotential  $X_0 \cdot f(X)$  would be  $U(1)^r$ -invariant:

$$q_{a0} + \sum_{i=1}^{n+r} q_{ai} = 0, \quad \text{for each } a = 1, \dots, r. \quad (1.4)$$

In the low-energy regime, the  $X_0$  field indeed behaves as a Lagrange multiplier, enforcing the constraint  $f(X) = 0$ —in the so-called “geometric” phases; see below. This gives the first hints about the geometry of the so-described target spaces, to be regarded as hypersurfaces  $\{f(X) = 0\} \subset A$ —which provides the technical-ease bias towards “well-known” ambient spaces,  $A$ ; see footnote 8.

<sup>8</sup>One seeks to work in a space where one knows just about everything one needs for the purposes of computing the desired characteristics and properties of the subspaces of interest; for starters, see Ref. [18].

**Remark 1.1:** The (1) superpotential gauge invariance condition (1.4) also (2) guarantees the anomaly cancellation for each  $U(1)$  gauge symmetry and is also (3) the condition for the ground-state hypersurface  $\{f(x) = 0\} \subset (\{X_i\}/U(1)^r)$  to have a vanishing 1st Chern class, and so (4) admit a Ricci-flat Kähler metric—to be a Calabi–Yau hypersurface.  $\blacksquare$

After integrating out the “auxiliary fields” (the equations of motion of which are algebraic, non-dynamical), the effective Lagrangian density contains the potential that is the sum of positive semi-definite terms:

$$\underbrace{\sum_a \left( \sum_i q_{ai} |X_i|^2 - t_a \right)^2}_{D\text{-terms}} + \underbrace{|f(X)|^2 + |X_0|^2 \sum_i \left| \frac{\partial f}{\partial X_i} \right|^2}_{F\text{-terms}} + \underbrace{\sum_a |\sigma_a|^2 \sum_i q_{ai}^2 |X_i|^2}_{\text{mixed terms}}. \quad (1.5)$$

The ground state is therefore determined by the vanishing of each summand, which are usually analyzed in turn and as provided in (1.5); see, e.g., [55]. Here we discuss in detail the choice of  $f(X)$ , in a concrete, showcasing example and complementing [55–59], rather than attempting to specify a general, and invariably rather complex meticulous algorithm.

In this framework, the geometry (metric) of the target space—spanned by the ground state degrees of freedom—emerges only through iterative computations in an interplay between so-called  $D$ -  $F$ - and mixed terms (1.5). In particular, gauge symmetry identifications result in the  $X^\mu(\xi)$ -space spanning a  $U(1; \mathbb{C})^r$  gauge-quotient, which induces much of its nontrivial topology and phase structure. Without the gauge-quotient, the minima of the potential would form a contractible cone of well-nigh trivial topology. The manifold variations in gauge-quotienting and choices of  $f(X)$ , however, makes the myriads of possible potentials (1.5) yield an embarrass of riches in the variety of topology and geometry of stringy spacetimes, which is regarded as both the boon and the bane in string theory—depending on whom one asks. In a rather welcome and marvelous turn of fate, the accelerating development of various computer-intensive methods and techniques (neural networks, machine-learning, artificial intelligence, . . .) of the past decade by now enables the computing, and with fast-increasing accuracy and breadth, the metric (and other characteristic quantities<sup>9</sup>) on Calabi–Yau manifolds, which until recently had to be analyzed without this explicit knowledge.

**Remark 1.2:** The worldsheet supersymmetry in the 1+1-dimensional (QFT) sigma models of interest protects the superpotential from renormalization. This makes it possible to completely omit it, whereupon the GLSM simply describes the embedding space as the gauge-quotient,  $\{X_i\}/U(1)^r$ , which we address in § 2—relying on the physics/QFT aspects and by switching to the concrete showcasing sequence of examples for simplicity.  $\blacksquare$

## 2 Gauge-Quotient Phases of the Showcasing Sequence

Certainly the best-known example of a convenient ambient space in which to construct subspaces of interest is the complex projective space,  $\mathbb{P}^n$ , encoded for toric geometry purposes [26–31] by the fan of complex multiples of the generating vectors,  $\nu_i$ :

$$\Sigma_{\mathbb{P}^n} = \left\{ \nu_i = \hat{e}_i, \quad i = 1, \dots, n, \quad \text{and} \quad \nu_{n+1} = - \sum_i \hat{e}_i \right\} \quad (2.1)$$

<sup>9</sup>Along with various aspects of curvature, the Ricci-flat metric on Calabi–Yau spaces is, as of recent, becoming increasingly more accessible via machine learning [91], so analyses such as presented herein should aim for complementary and streamlining insight. The rapidly growing literature on the subject is itself fascinating and would take us too far afield to provide an even remotely fair and functional review; suffice it here to direct the reader to the relatively recent works [33–38, 91] and references therein for starters.

This (**0**-centered) fan is generated by  $n+1$  vectors, each corresponding to a complex (homogeneous) coordinate,  $\nu_i \mapsto X_i \in \mathbb{C}$ , on which the single  $\mathbb{C}^* \approx U(1; \mathbb{C})$  symmetry acts isotropically:  $X_i \simeq \lambda^1 X_i$ . In the GLSM, this  $U(1)$  is gauged, turning the field space into the very well studied  $U(1; \mathbb{C}) \approx \mathbb{C}^*$  gauge-quotient; see [92] and references therein.

Following Ref. [54–59], we recall the definition of Hirzebruch  $n$ -fold scrolls:

**Definition 2.1** (Hirzebruch  $n$ -folds): *Hirzebruch  $n$ -folds are defined, **equivalently**, as:*

1. the **projective bundle**,  $F_m^{(n)} := \mathbb{P}(\mathcal{O}_{\mathbb{P}^1}(m) \oplus \mathcal{O}_{\mathbb{P}^1}^{\oplus(n-1)})$ ,
2. an  $m$ -**twisted  $\mathbb{P}^{n-1}$ -bundle over  $\mathbb{P}^1$** , and
3. the **bi-projective hypersurface**,  $\{p_0(x, y) := x_0 y_0^m + x_1 y_1^m = 0\} \subset \mathbb{P}_x^n \times \mathbb{P}_y^1$ .

Each such  $n$ -fold also has a toric rendition:

4. the **toric variety**, itself defined up to  $\mathrm{GL}(n, \mathbb{Z})$  lattice transformations by the  $n$ -dimensional **fan** spanned by the vectors

$$\Sigma_{F_m^{(n)}} = \left\{ \nu_1 := -\sum_{i=1}^{n-1} \hat{e}_i, \quad \underbrace{\nu_{k+1} := \hat{e}_k}_{k=1, \dots, n}, \quad \nu_{n+2} := -m \sum_{i=1}^{n-1} \hat{e}_i - \hat{e}_n \right\} \quad (2.2)$$

where  $\{\nu_1, \dots, \nu_n\}$  span the fiber- $\mathbb{P}^{n-1}$ , and  $\{\nu_{n+1}, \nu_{n+2}\}$  the base- $\mathbb{P}^1$ .

The  $n = 2$  examples,  $F_m^{(2)}$ , are the well-known Hirzebruch surfaces [77], seen to be a minor modification (at  $\nu_1$  and  $\nu_{n+2}$ ) of  $\Sigma_{\mathbb{P}^n}$  (2.1): The fan  $\Sigma_{F_m^{(n)}}$  (2.2) is generated  $n+2$  vectors, has as many complex (Cox) coordinates, and so encodes a  $U(1; \mathbb{C})^2$ -quotient, one of each  $U(1; \mathbb{C})$ 's “inherited” from the fiber- $\mathbb{P}^{n-1}$  and the base- $\mathbb{P}^1$ ; this will be made precise in §3.

This variety of equivalent definitions and widespread use and study of these varieties in diverse sub-fields of algebraic geometry provides for computational versatility, which makes them exceptionally appealing as “well-known” ambient spaces; see footnote 8. The computational aspects of this goal benefit from the coordinate-level identification between the bi-projective embedding (item 3) and the toric specification (item 4) [56–59].

The particular choice of vectors (2.2) in fact encodes the  $U(1; \mathbb{C})^2$ -charges of  $X_i$  by way of the relation

$$\sum_{i=1}^{n+2} q_a(X_i) \nu_i = -q_a(X_0), \quad q_{ai} := q_a(X_i), \quad (2.3)$$

resulting in the structure tabulated here for  $n = 3$ :

$n = 3$	$\nu_0$	$\nu_1$	$\nu_2$	$\nu_3$	$\nu_4$	$\nu_5$
$\Sigma_{F_m^{(3)}} \left\{ \begin{array}{l} 0 \\ 0 \\ 0 \end{array} \right.$	0	-1	1	0	0	- $m$
	0	-1	0	1	0	- $m$
	0	0	0	0	1	-1
	1	0	0	0	0	0
$q_1$	-3	1	1	1	0	0
$q_2$	$(m-2)$	- $m$	0	0	1	1
$q_3$	$-2(m+1)$	0	$m$	$m$	1	1
$q_4$	0	$-2(m+1)$	$(m-2)$	$(m-2)$	3	3
<b>Cox variables:</b>	$X_0$	$X_1$	$X_2$	$X_3$	$X_4$	$X_5$

(2.4)

The generators  $\nu_i$  are given as column 3-vectors and the origin,  $\nu_0$ , is associated with the Lagrange-multiplier-like,  $X_0$ . All  $q_1, \dots, q_4$  satisfy: **(a)** their defining equation (2.3), **(b)** the key (Calabi–Yau) requirement (1.4), and are chosen so as to vanish for (at least) one of the  $X_i$ —which will be needed below.

(c) Any two of the four 6-vectors,  $q_a$ , are linearly independent and provide an a priori equally valid  $U(1)^2$ -charge basis. (d) Any two of these 6-vectors,  $(q_{a0}, \dots, q_{a5})$  stacked underneath the 3+1 rows of  $\nu_0, \dots, \nu_5$  form a regular  $6 \times 6$  matrix,<sup>10</sup> so these six rows and six columns form six linearly independent 6-vectors. (e) The same holds if one omits the 4th, separated row in (2.4) and the  $\nu_0$ -column, which corresponds to the fiber of the anticanonical bundle of  $F_m^{(n)}$ . Being a unit distance *above* the origin,  $\mathbf{0}$ , in the  $(n+1)^{\text{th}}$  direction,  $\nu_0$  is the apex of a pyramid *over* the “base” spanned by  $\{\nu_1, \dots, \nu_{n+2}\}$  in a  $\mathbb{Z}^n$ -lattice in the real  $n$ -space,  $(\mathbb{Z}^n \otimes_{\mathbb{R}} \mathbb{R}^n)$ —encoding the fiber of the anticanonical bundle over  $F_m^{(n)}$ . Standard (complex-algebraic) toric geometry identifies  $q_1, q_2$  as the *Mori vectors* of  $F_m^{(n)}$ ,  $q_3$  being their non-negative linear combination [27, 30, 93]; the linear combination  $q_4 = (m-2)q_1 + nq_2$  is also non-negative for  $m \geq 2$ .

## 2.1 Field Space Gauge-Orbits

Since the field space spanned by the  $X_i$  is in fact a  $U(1; \mathbb{C})^2$ -gauge quotient, and the  $U(1; \mathbb{C})^2$ -transformation of  $(X_0; X_1, \dots, X_5) \in \mathbb{C}^6$  is evidently not uniform, one must apportion (*stratify*) the affine field-space,  $\mathbb{C}^6$ , into regions of uniform  $U(1; \mathbb{C})^2$ -transformation (gauge-orbits) to specify a well-defined quotient.

**The  $\mathbb{P}^n$  Template:** For a simple example (2.1), the group of all complex nonzero rescalings

$$\mathbb{C}^2 \ni (z_1, z_2) \mapsto \lambda \cdot (z_1, z_2) := (\lambda z_1, \lambda z_2) \in \mathbb{C}^2, \quad (\lambda \neq 0) \in \mathbb{C}^* \approx U(1; \mathbb{C}), \quad (2.5)$$

is *free* on the subset  $((z_1, z_2) \neq (0, 0)) \in \mathbb{C}^2$ , since  $\lambda(z_1, z_2) = \lambda'(z_1, z_2)$ , implies that  $\lambda = \lambda'$ . The  $\mathbb{C}^*$ -transformation (2.5) clearly fails to be *free* at the origin,  $\mathbf{E}_o := (0, 0) \in \mathbb{C}^1$ —which alone is *fixed* by (invariant under) the  $\mathbb{C}^*$ -transformation (2.5). When constructing “ $\mathbb{C}^*$ -gauge quotients,” one must separate these two  $\mathbb{C}^*$ -orbits and their respective quotients (“ $\sqcup$ ” denotes disjoint union):

$$\mathbb{C}^2 / \mathbb{C}^* \rightsquigarrow ((\mathbb{C}^2 \setminus \mathbf{E}_o) / \mathbb{C}^*) \sqcup \mathbf{E}_o / \mathbb{C}^* = \mathbb{P}^1 \sqcup \mathbf{E}_o. \quad (2.6)$$

Although the region  $(\mathbb{C}^2 \setminus \{(0, 0)\}) \subset \mathbb{C}^2$  that results in the quotient  $\mathbb{P}^1$  includes points that are infinitesimally near the other region,  $(0, 0) \in \mathbb{C}^2$ , the resulting quotients  $\mathbb{P}^1$  and  $(0, 0)$  are well separated, and the  $(z_1, z_2) \in \mathbb{C}^2$  space has been partitioned into two  $U(1; \mathbb{C})$ -orbits (2.6): one (complex) 1-dimensional, the other 0-dimensional.

In general, denote by  $\mathbf{E} \dots$  the fixed-point locus of a  $\mathbb{C}^*$ -transformation such as in (2.5)–(2.6).

► **The  $F_m^{(2)}$  Sequence:** In the showcase models (2.2), the gauge symmetries,  $U_a(1)$ , act with charges  $q_a$  given as in (2.4) on (complex) chiral superfields and so equally on their lowest, scalar component fields,  $X_0, X_1, \dots, X_{n+2}$ :

$$U_1(1; \mathbb{C}): (\lambda_1^{-n} X_0, \lambda_1 X_1, \lambda_1 X_2, \dots, \lambda_1 X_n; \underline{X_{n+1}}, \underline{X_{n+2}}), \quad (2.7a)$$

$$U_2(1; \mathbb{C}): (\lambda_2^{m-2} X_0, \lambda_2^{-m} X_1, \underline{X_2}, \dots, \underline{X_n}; \lambda_2 X_{n+1}, \lambda_2 X_{n+2}), \quad (2.7b)$$

$$U_3(1; \mathbb{C}): (\lambda_3^{-[(n-1)m+2]} X_0, \underline{X_1}, \lambda_3^m X_2, \dots, \lambda_3^m X_n; \lambda_3 X_{n+1}, \lambda_3 X_{n+2}), \quad (2.7c)$$

$$U_4(1; \mathbb{C}): (\underline{X_0}, \lambda_4^{-[(n-1)m+2]} X_1, \lambda_4^{m-2} X_2, \dots, \lambda_4^{m-2} X_n; \lambda_4^n X_{n+1}, \lambda_4^n X_{n+2}), \quad (2.7d)$$

where the  $U_a(1)$ -neutral fields have been underlined: Their nonzero *vacuum expectation values* (abbreviated “vev”s) leave that particular  $U_i(1)$  unbroken; these vev’s specify the different choices of a “classical background” and so also the broken-vs.-unbroken gauge symmetry in those “phases.”

Extending the example (2.5)–(2.6), these (toric) actions define special subsets of the field space, by separating regions that are fixed by these  $\mathbb{C}^*$ -transformations from the complement that is being  $\mathbb{C}^*$ -rescaled. The tabulation of charges (2.4) and the complexified (toric) actions (2.7a)–(2.7d) make it evident

<sup>10</sup>For  $F_m^{(n)}$ , the determinant of this matrix is  $(-1)^{n+1} (2n + (n-1)m^2)$ .

that the field space should be regarded as the tensor product of the factors fixed by the indicated rank-1 subgroups of the  $U(1; \mathbb{C})^2$  gauge group:

<b>Factor</b>	$\mathbb{C}_0^1 = \{X_0\}$	$\mathbb{C}_1^1 = \{X_1\}$	$\mathbb{C}_2^{n-1} = \{X_2, \dots, X_n\}$	$\mathbb{C}_3^2 = \{X_{n+1}, X_{n+2}\}$	
<b>Fixed by</b>	$U_4(1; \mathbb{C})$	$U_3(1; \mathbb{C})$	$U_2(1; \mathbb{C})$	$U_1(1; \mathbb{C})$	(2.8)
<b>Excep. set</b>	$\mathbf{E}_0 = (0)$	$\mathbf{E}_1 = (0)$	$\mathbf{E}_2 = (0, \dots, 0)$	$\mathbf{E}_3 = (0, 0)$	

Underneath each factor are listed also the “exceptional sets” [30, p. 207], each of which is actually fixed (as a subset of its factor,  $\mathbf{E}_I \subset \mathbb{C}_I^{d_I}$ , indicated at the top of its column in (2.8)) by all of  $U(1; \mathbb{C})^2$ . Indeed, the only location in the full field space,  $\mathbb{C}_{0123}^{n+3}$ , that is fixed (left invariant) by the full  $U(1; \mathbb{C})^2$  gauge symmetry is the field-space origin:

$$\begin{aligned} \mathbf{E}_{0123} &:= \mathbf{E}_0 \boxtimes \mathbf{E}_1 \boxtimes \mathbf{E}_2 \boxtimes \mathbf{E}_3 = (0; 0, 0, \dots, 0; 0, 0) \in \mathbb{C}_{0123}^{n+3}, \\ &= \{X_0 = 0\} \boxtimes \{X_1 = 0\} \boxtimes \{X_2, \dots, X_n = 0\} \boxtimes \{X_{n+1} = 0 = X_{n+2}\}, \\ &= \{X_0 = 0 \ \& \ X_1 = 0 \ \& \ X_2, \dots, X_n = 0 \ \& \ X_{n+1} = 0 = X_{n+2}\}, \end{aligned} \quad (2.9)$$

where “ $\boxtimes$ ” is the tensor product, however, with the logical *conjunction* of the defining relations implied, as specified in the last row. Analogously,

$$\begin{aligned} (\mathbf{E}_{12} &:= \{X_1 = 0\} \boxtimes \{X_2, \dots, X_n = 0\} = \{X_1, \dots, X_n = 0\}) & (2.10) \\ &\subset \mathbb{C}_{12}^n := \mathbb{C}_1^1 \boxtimes \mathbb{C}_2^{n-1}, \end{aligned}$$

$$\begin{aligned} (\mathbf{E}_{23} &:= \{X_2, \dots, X_n = 0\} \cap \{X_{n+1} = 0 = X_{n+2}\} = \{X_2, \dots, X_{n+2} = 0\}) & (2.11) \\ &\subset \mathbb{C}_{23}^{n+1} := \mathbb{C}_2^n \boxtimes \mathbb{C}_3^2, \end{aligned}$$

and so on. (When viewed as subsets of the *full* field space,  $\mathbb{C}_{0123}^{n+3}$ , the defining relations of each exceptional set (2.8) leaves the complementary factors unrestricted, so that

$$(\overline{\mathbf{E}_{12}} \subset \mathbb{C}_{0123}^{n+3}) := (X_0; 0, 0, \dots, 0; X_{n+1}, X_{n+2}) = \mathbf{E}_{12} \otimes \mathbb{C}_{03}^3; \quad (2.12)$$

$$(\overline{\mathbf{E}_{23}} \subset \mathbb{C}_{0123}^{n+3}) := (X_0; X_1, 0, \dots, 0; 0, 0) = \mathbf{E}_{23} \otimes \mathbb{C}_{01}^2; \quad \text{etc.} \quad (2.13)$$

Then,  $\mathbf{E}_{0123} = \mathbf{E}_0 \boxtimes \mathbf{E}_1 \boxtimes \mathbf{E}_2 \boxtimes \mathbf{E}_3 = \overline{\mathbf{E}_0} \cap \overline{\mathbf{E}_1} \cap \overline{\mathbf{E}_2} \cap \overline{\mathbf{E}_3}$ .)

► *Gauge-Equivalence Strata:* (I) Omitting  $X_0$ , we see that for example:

$$\left( \underbrace{((\mathbb{C}_{12}^n \setminus \mathbf{E}_{12})/U_1(1; \mathbb{C})) \times (\mathbb{C}_3^2 \setminus \mathbf{E}_3)}_{= \mathbb{P}_{\text{fiber}}^{n-1}} \right) / U_2(1; \mathbb{C}) \simeq F_m^{(n)} \quad (2.14)$$

where  $U_2(1; \mathbb{C})$  projectivizes  $\mathbb{C}_3^2 \setminus \mathbf{E}_3 \rightarrow \mathbb{P}_{\text{base}}^1$  while also  $m$ -twisting<sup>11</sup>  $\mathbb{P}_{\text{fiber}}^{n-1}$ . This then describes an  $m$ -twisted  $\mathbb{P}_{\text{fiber}}^{n-1}$ -bundle over  $\mathbb{P}_{\text{base}}^1$ , the Hirzebruch  $n$ -fold scroll,  $F_m^{(n)}$ .

(II) Alternatively, we also have:

$$\left( (\mathbb{C}_1^1 \setminus \mathbf{E}_1) \times \underbrace{((\mathbb{C}_{23}^{n+1} \setminus \mathbf{E}_{23})/U_3(1; \mathbb{C}))}_{= \mathbb{P}_{(m:\dots:m:1:1)}^n} \right) / U_2(1; \mathbb{C}), \quad (2.15)$$

<sup>11</sup>The  $U_2(1)$ -transformation is trivial on  $\mathbb{P}_{\text{base}}^1 \ni (X_{n+1}, X_{n+2}) \simeq (\lambda X_{n+1}, \lambda X_{n+2})$ , but is a non-trivial coordinate reparametrization on  $\mathbb{P}_{\text{fiber}}^{n-1} \ni (X_1, X_2, \dots, X_n) \not\simeq (\lambda_2^{-m} X_1, X_2, \dots, X_n)$ .

which describes a blowup of  $\mathbb{P}_{(m:\dots:m:1:1)}^n$  along  $(X_2, \dots, X_n; 0, 0)$  and parametrized by  $X_1$ . This codimension-2 linear subspace is fixed by the discrete subgroup  $\mathbb{Z}_m \subset U_3(1; \mathbb{C})$ , which may be seen as follows: The linear subset

$$S = ((X_2, \dots, X_n; 0, 0)/U_3(1; \mathbb{C})) \subset \mathbb{P}_{(m:\dots:m:1:1)}^n \quad (2.16)$$

is fixed by the  $\mathbb{Z}_m \subset U_3(1; \mathbb{C})$

$$U_3(1; \mathbb{C}) \supset \mathbb{Z}_m: (\lambda_3^m X_2, \dots, \lambda_3^m X_n; 0, 0), \quad \lambda_3^m = 1, \quad (2.17)$$

and is a  $\mathbb{Z}_m$ -singular locus in  $\mathbb{P}_{(m:\dots:m:1:1)}^n$ . Subsequently, the  $U_2(1; \mathbb{C})$ -transformation separates:

$$(\mathbb{C}_1^1 = \{X_1 \in \mathbb{C}\}) \times S \rightarrow (\{X_1 = 0\} \times S) \sqcup (\{X_1 \neq 0\} \times S), \quad (2.18)$$

as the trivial and non-trivial  $U_2(1; \mathbb{C})$ -orbits, respectively. The former of these leaves the  $X$ -space  $\mathbb{Z}_m$ -singular at  $S$  and identified as the singular weighted projective space  $\mathbb{P}_{(m:\dots:m:1:1)}^n$ ; the latter provides its MPCP-desingularization [48] of along  $S$ .

Since  $U_1(1; \mathbb{C}) \times U_2(1; \mathbb{C}) \approx U_3(1; \mathbb{C}) \times U_2(1; \mathbb{C})$ , the iterated quotient (2.15) is isomorphic to (2.14), thus giving the Hirzebruch  $n$ -fold,  $F_m^{(n)}$ , one more alternative description as the MPCP-desingularization of the weighted  $\mathbb{P}_{(m:\dots:m:1:1)}^n$ .

The above two choices, **I** (2.14) and **II** (2.15), correspond to the two “geometric” phases. Replacing the complements  $(\mathbb{C}_1^d \setminus \mathbf{E} \dots)$  of the fixed-loci with the fixed loci  $\mathbf{E} \dots$  themselves, and combinatorially in the various factors of (2.14) and (2.15), gives the “complementary” strata in the field space:

$$\text{III} : [F_m^{(n)}]_{\text{LGO}} : \left( (\mathbb{C}_1^n \setminus \mathbf{E}_1) \times ((\mathbf{E}_{23})/U_3(1; \mathbb{C})) \right) / U_2(1; \mathbb{C}), \quad (2.19)$$

$$\text{IV} : [F_m^{(n)}]_{\text{hyb.}} : \left( [(\mathbf{E}_{12})/U_1(1; \mathbb{C})] \times (\mathbb{C}_3^2 \setminus \mathbf{E}_3) \right) / U_2(1; \mathbb{C}). \quad (2.20)$$

Writing  $\mathbf{E}_{\dots}^c := (\mathbb{C}_{\dots} \setminus \mathbf{E} \dots)$  for the complement of the exceptional set, the (complexified) gauge symmetries reduce the field-space to the  $U(1; \mathbb{C})^2$ -equivalence classes in the following four field-space regions:

$$\begin{array}{l} \text{phase IV} = [\mathbf{E}_0^c \times \mathbf{E}_{12} \times \mathbf{E}_3^c] \quad [\mathbf{E}_0 \times \mathbf{E}_{12}^c \times \mathbf{E}_3] = \text{phase I} \\ \text{phase III} = [\mathbf{E}_0^c \times \mathbf{E}_1^c \times \mathbf{E}_{23}] \quad [\mathbf{E}_0 \times \mathbf{E}_1 \times \mathbf{E}_{23}^c] = \text{phase II} \end{array} \quad (2.21)$$

where the  $\mathbb{C}_0^1$  factor is now also included. The (red) dotted arrows indicate the (dimensional) collapse  $\mathbf{E}_i^c \rightarrow \mathbf{E}_i$ , from the complement of the (gauge-fixed) exceptional set to the exceptional set itself. The plain (blue) solid lines trace unchanged factors in the tensor product.

The diagram (2.21) presents the field space,  $(X_0, X_1, \dots, X_{n+2}) \in \mathbb{C}^{n+3}/U(1)^2$ , decomposed into four distinct regions, labeled as “phases” (adopting the by now standard nomenclature [19]). From (2.8) and (2.21), we have:

$$\begin{array}{c|cccc} I & 0 & 1 & 2 & 3 \\ \hline \dim(\mathbf{E}_I) & 0 & 0 & 0 & 0 \\ \dim(\mathbf{E}_I^c) & 1 & 1 & n-1 & 2 \end{array} \Rightarrow \begin{array}{c|cccc} \text{phase} & \text{I} & \text{II} & \text{III} & \text{IV} \\ \hline \dim & n & n & 0 & 1 \end{array} \quad (2.22)$$

where quotienting by  $U(1)^2$  reduces the dimension-count to those tabulated at right.

As in Ref. [19], the variable  $X_0$  is seen to provide a fiber-coordinate for a degree- $\binom{n}{2-m}$  line bundle over  $F_m^{(n)}$ , which is set to zero in phases I and II, these describing the Calabi-Yau hypersurface in the base space,  $F_m^{(n)}[c_1]$ . In phase III, the base of the bundle collapses to  $\mathbf{E}_{23} = \{\text{pt.}\}$  and  $|X_1| = \sqrt{\frac{(2-m)r_1 - nr_2}{(n-1)m+2}}$  while  $|X_0| = \sqrt{\frac{-mr_1 - r_2}{(n-1)m+2}}$ . Finally, in phase IV, the bundle collapses to  $\mathbf{E}_{12} \times \mathbb{P}_{\text{base}}^1$  and  $|X_0| = \sqrt{-r_1/n}$ .

Complementing the analysis in Ref. [55], the above detailed  $U(1)^2$  gauge-orbit separation (stratification) shows that, far from a simple  $(X_0, X_1, \dots, X_5) \in \mathbb{C}^6$ , the field space has a rather intricate structure: This rather straightforward if detailed QFT reasoning thus fully recovers the complex-algebraic toric geometry-standard Gelfand–Kapranov–Zelevinsky (GKZ) decomposition [94]; see below, and compare also with Refs. [19, 20, 55].

## 2.2 VEVs and Phases

Having stratified the field space into uniform  $U(1)^2$ -orbits, consider now the possible choices of ground-state vev's, which maintain the vanishing of the potential (1.5). In particular, with the  $(q_1, q_2)$ -basis in (2.4), the vanishing of the “ $D$ -terms” implies:

$$\left(-n|X_0|^2 + \sum_{i=1}^n |X_i|^2 - t_1\right) \stackrel{!}{=} 0, \quad (2.23a)$$

$$\left((m-2)|X_0|^2 - m|X_1|^2 + \sum_{j=1}^2 |X_{n+j}|^2 - t_2\right) \stackrel{!}{=} 0, \quad (2.23b)$$

where “ $\stackrel{!}{=}$ ” denotes a required equality. Note that these equations are independent of the choice of the superpotential, and so in fact describe the ambient space,  $F_m^{(n)}$ , itself.

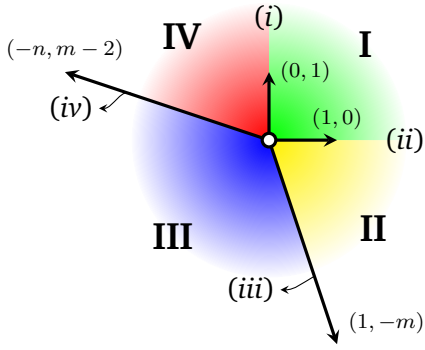
Depending on the values of the so-called “Fayet-Iliopoulos” couplings,  $(t_1, t_2)$ , the following options emerge (following [20, 55])—fully consistent with (2.7) above:

- (i)  $U_1(1)$  is preserved if  $X_{n+1}, X_{n+2} \neq 0$  but  $X_0 = 0 = X_i$  for  $i = 1, \dots, n$ . Since  $\text{LCM}[q_2(X_i)] = 1$ ,  $U_2(1)$  is broken completely. In this case (2.23a) and (2.23b) imply:  $t_1 = 0$  and  $t_2 \geq 0$ ; this is the positive  $(0, 1)$ -direction in the  $(t_1, t_2)$ -plane.
- (ii)  $U_2(1)$  is preserved if  $X_2, \dots, X_n \neq 0$  but  $X_0 = 0 = X_1 = X_{n+1} = X_{n+2}$ . Since  $\text{LCM}[q_1(X_0, X_1, X_{n+1}, X_{n+2})] = 1$ ,  $U_1(1)$  is broken completely. Now (2.23b) and (2.23a) imply:  $t_2 = 0$  and  $t_1 \geq 0$ , along the positive  $(1, 0)$ -direction.
- (iii)  $U_3(1)$  is preserved if only  $X_1 \neq 0$ . Since  $q_1(X_1) = 1$ ,  $U_1(1)$  is broken completely, but  $q_2(X_1) = -m$  implies  $U_2(1) \rightarrow \mathbb{Z}_m$  and  $q_4(X_1) = -(n-1)m-2$  implies  $U_4(1) \rightarrow \mathbb{Z}_{(n-1)m+2}$ . Now (2.23b) and (2.23a) imply:  $mt_1 + t_2 = 0$ , along the positive  $(1, -m)$ -direction.
- (iv)  $U_4(1)$  is preserved if only  $X_0 \neq 0$ . Since  $q_1(X_0) = -n$ ,  $U_1(1) \rightarrow \mathbb{Z}_n$ ,  $q_2(X_0) = m-2$  implies  $U_2(1) \rightarrow \mathbb{Z}_{m-2}$  and  $q_3(X_0) = -(n-1)m-2$  implies  $U_3(1) \rightarrow \mathbb{Z}_{(n-1)m+2}$ . Now (2.23b) and (2.23a) imply:  $(m-2)t_1 + nt_2 = 0$ , along the positive  $(-n, (m-2))$ -direction.

Summarizing, we have found demarcation rays in the Fayet-Iliopoulos  $(t_1, t_2)$ -space generated by:

$$\begin{array}{c|cccc} & \text{(i)} & \text{(ii)} & \text{(iii)} & \text{(iv)} \\ \hline \begin{pmatrix} t_1 \\ t_2 \end{pmatrix} & \begin{pmatrix} 0 \\ 1 \end{pmatrix} & \begin{pmatrix} 1 \\ 0 \end{pmatrix} & \begin{pmatrix} 1 \\ -m \end{pmatrix} & \begin{pmatrix} -n \\ m-2 \end{pmatrix} \end{array} \quad (2.24)$$

which are *precisely* the distinct (vertically read) 2-vectors appearing in the  $(q_1, q_2)$ -rows in the tabulation (2.4)! The preceding  $U(1)^2$ -stratification (2.21) thus *precisely* reproduces the vev-analysis [19, 20, 55] and the phase-diagram in Figure 1, also known as the GKZ decomposition [94]. With the specified demar-



- Only the (iv) demarcation depends on  $n = \dim(F_m^{(n)})$ .
- Only the (iii) and (iv) demarcations depend on the “twist,”  $m$ .
- The (ii) and (iii) demarcations coincide for  $m = 0$ , removing phase II.

**Figure 1:** The  $F_m^{(n)}[c_1]$  GLSM “phase diagram,” plotted here for  $n = 3$  and  $m = 3$ .

cations, Eqs. (2.23) determine the actual values of the nonzero vevs (omitting the usual  $\langle \dots \rangle$  notation and correcting [55, Fig. 1]); see Table 1, where two of the vevs, in phases II and VI, are:

$$|X_1|_{\text{II}} = \sqrt{t_1 - \sum_{i=2}^n |X_i|^2} \geq 0, \quad |X_0|_{\text{IV}} = \sqrt{\frac{|X_{n+1}|^2 + |X_{n+2}|^2 - t_1}{n}}. \quad (2.25)$$

The vevs change continuously throughout the  $(t_1, t_2)$ -plane. The particular  $q_a$ -choices in (2.4) are thus

**Table 1:** The vacuum expectation (background) values of the various fields in the various phases of the  $F_m^{(n)}[c_1]$  GLSM.

	$ X_0 $	$ X_1 $	$ X_2  \cdots  X_n $	$ X_{n+1} $	$ X_{n+2} $
<b>i</b>	0	0	0 $\cdots$ 0	*	*
<b>I</b>	0	*	* $\cdots$ *	*	*
<b>ii</b>	0	0	* $\cdots$ *	0	0
<b>II</b>	0	see (2.25)	* $\cdots$ *	*	*
<b>iii</b>	0	$\sqrt{t_1}$	0 $\cdots$ 0	0	0
<b>III</b>	$\sqrt{\frac{-mt_1 - t_2}{(n-1)m+2}}$	$\sqrt{\frac{(2-m)t_1 - nt_2}{(n-1)m+2}}$	0 $\cdots$ 0	0	0
<b>iv</b>	$\sqrt{-t_1/n}$	0	0 $\cdots$ 0	0	0
<b>IV</b>	see (2.25)	0	0 $\cdots$ 0	*	*

“\*” denotes nonzero values; all vevs vanish at  $(t_1, t_2) = (0, 0)$ .

seen as particularly convenient for determining the  $U(1; \mathbb{C})^2$  gauge-symmetry breaking pattern throughout the phase diagram in Figure 1, as induced by the values provided in Table 1. Since  $q_3$  and  $q_4$  are linear combinations of  $q_1$  and  $q_2$ , the above analysis can be re-done using any of the  $\binom{4}{2} = 6$  bases of any two of  $q_1, \dots, q_4$ , resulting in the same phase diagram, up to a  $\text{GL}(2; \mathbb{Z})$ -transformation. Quite literally then, all  $\binom{4}{2} = 6$   $q_a$ -bases are physically equivalent, whereas built-in positivity requirements in complex-algebraic toric geometry single out the Mori vectors,  $(q_1, q_2)$ .

The infinite sequence  $(m = 0, 1, 2, \dots)$  of Hirzebruch surface (complex 2-dimensional) scrolls,  $F_m^{(2)}$ , is well-known to provide only two diffeomorphism classes [25, 27–30, 77, 78]: the even-twisted  $F_{2k}^{(2)}$  are all diffeomorphic to each other (“same, as smooth real manifolds”), as are the odd-twisted  $F_{2k+1}^{(2)}$ . We may write  $F_m^{(2)} \approx_{\mathbb{R}} F_{m \pmod{2}}^{(2)}$ , and find that  $F_m^{(n)} \approx_{\mathbb{R}} F_{m \pmod{n}}^{(n)}$  analogously [55]. In turn, the  $F_m^{(n)}$  for differing  $m$  are all distinct as complex manifolds, and this is clearly seen from the phase diagrams in Figure 1, reproduced in Figure 2 for  $n = 3$  and for  $m = 0, 1, \dots, 4$ . The sequence of Hirzebruch scrolls is in fact infinite, with the  $\mathbb{P}^{n-1} \hookrightarrow F_m^{(n)} \rightarrow \mathbb{P}^1$  bundle twist,  $m$ , unbounded. In fact, as the next section shows, there is an additional diversity for  $n \geq 3$  that is growing combinatorially with  $m$ .

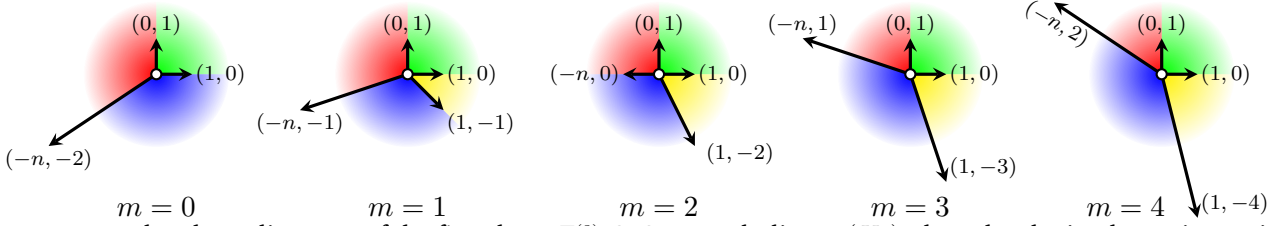


**Figure 2:** The phase diagrams of the first three  $F_m^{(3)}$ -GLSMs. Including  $q_a(X_0)$ , they also depict the anticanonical bundles,  $\mathcal{K}_{F_m^{(n)}}^*$ , sections of which define Ricci-flat hypersurfaces as their zero locus

The  $m$ -dependent characteristic that unequivocally distinguishes the various Hirzebruch scrolls,  $F_m^{(n)}$ , is their hallmark *exceptional divisor* (complex codimension-1 irreducible submanifold),  $\mathcal{S} \subset_{\mathbb{C}} F_m^{(n)}$ , called the *directrix* [25] and being identified by its maximally negative self-intersection:  $[\mathcal{S}]^n = -(n-1)m$ . The Ricci-flat (Calabi–Yau) hypersurfaces  $\mathcal{X} \subset F_m^{(n)}$  themselves being of complex codimension-1 therefore intersect this  $\mathcal{S}$ :

$$\dim(\mathcal{X} \subset F_m^{(n)}) = n-1, \quad \Rightarrow \quad \dim((\mathcal{X} \cap \mathcal{S}) \subset F_m^{(n)}) = n-2, \quad (2.26)$$

and so “inherit” the distinguishing features stemming from  $\mathcal{S} \subset F_m^{(n)}$ ; those loci naturally turn up in  $H_{n-2}(\mathcal{X}, \mathbb{Z})$ , and so provide a relevant distinction in stringy applications.

In contradistinction, the phase diagrams in Figure 2 quite clearly *do not* exhibit the diffeomorphism 3-cycle,  $F_m^{(3)} \approx_{\mathbb{R}} F_{m \bmod 3}^{(3)}$ . Since these diagrams are defined only up to  $\mathrm{GL}(2; \mathbb{Z})$  basis transformations, one may wonder if perhaps their acyclic nature is a mirage. That this is not the case should be evident on comparing the  $m=0$  and  $m=3$  diagrams: the two cannot possibly be  $\mathrm{GL}(2; \mathbb{Z})$ -equivalent, since the former lacks phase II. It may be a little less evident that this in fact persists for any pair,  $F_m^{(2)}, F_{m'}^{(2)}$  with  $m' \neq m$ : Requiring the candidate  $\mathrm{GL}(2; \mathbb{Z})$ -transformation,  $\mathbf{g}$ , to map  $\{(\frac{1}{0}), (\frac{0}{1}), \dots\}_m \rightarrow \{(\frac{1}{0}), (\frac{0}{1}), \dots\}_{m'}$ , fixes  $\mathbf{g} = \mathbb{1}$ , which then cannot possibly map the remaining two demarcations,  $\{(-\frac{1}{m}), (\frac{-n}{2-m})\} \not\rightarrow \{(-\frac{1}{m'}), (\frac{-n}{2-m'})\}$ . This exhibits the inequivalence of  $F_m^{(n)}[c_1]$  GLSMs even at this semi-classical stage [19]! These differences only increase upon including also the cumulative worldsheet instanton effects, following [20].<sup>12</sup>

However, the phase diagrams (also known as “secondary fans,”  $\Sigma_{\mathcal{X}}''$ ) partition the Fayet–Iliopoulos  $t_a$ -space (parametrizing the  $U(1; \mathbb{C})^r$  gauge symmetry), and so parametrize not the complex structure, but the (complexified) *Kähler structure* [19, 20] of the ambient scrolls,  $F_m^{(n)}$ , and thus (properly restricted) also of the Ricci-flat hypersurfaces therein. By including the  $q_a(X_0) = (\frac{-n}{m-2})$  demarcation, they also refer to (the fiber of) the anticanonical class,  $\mathcal{K}_{F_m^{(n)}}^*$ , and so pertain to the deformation family anticanonical hypersurfaces,  $F_m^{(n)}[c_1]$ .

**Corollary 2.1:** *The  $\Sigma_{F_m^{(n)}}'' \not\approx \Sigma_{F_{m'}^{(n)}}''$  differences exhibited in Figure 2 characterize (the GLSM dependence on) the Kähler structure of the Hirzebruch scrolls, their anticanonical bundles, and so also their Ricci-flat (anticanonical, Calabi–Yau) hypersurfaces, throughout  $F_m^{(n)}[c_1]$ .*

### 3 Deformation Family of Ambient Spaces

The study of Calabi–Yau hypersurfaces in Hirzebruch scrolls benefits greatly from being able to provide a concrete realization of the hallmark exceptional divisor. This uses the novel technique of generalized hypersurfaces and their complete intersections [54, 95, 96], and then translates that into the complex-algebraic toric geometry framework. The (unbounded in  $m$ ) sequence of Hirzebruch scrolls,  $F_m^{(n)}$ , also harbors an additional diversity for  $n \geq 3$  that is growing combinatorially with  $m$ , which is exhibited in the biprojective embedding, and then organized and catalogued using the toric identifications.

<sup>12</sup>I am indebted to Per Berglund for collaboration on this result, which will be reported elsewhere.

### 3.1 Biprojective vs. Toric Renditions

**Biprojective Rendition:** Following [56, Construction 2.1] and [59], in every particular hypersurface

$$F_{m;\epsilon}^{(n)} := \{p_\epsilon(x, y) = 0\} \in \left[ \begin{array}{c} \mathbb{P}^n \\ \mathbb{P}^1 \\ m \end{array} \right], \quad (3.1a)$$

$$p_\epsilon(x, y) := x_0 y_0^m + x_1 y_1^m + \sum_{i=0}^n \sum_{\ell=1}^{m-1} \epsilon_{i\ell} x_i y_0^{m-\ell} y_1^\ell, \quad \epsilon_{i\ell} \in \mathbb{C}, \quad (3.1b)$$

one finds its collection of mutually *algebraically independent*<sup>13</sup> irreducible hypersurfaces,  $\{\mathcal{S}_\alpha := \{\mathfrak{s}_\alpha(x, y) = 0\} \subset F_m^{(n)}\}$ , each of maximally negative self-intersection, and explicitly constructed as generalized hypersurfaces. This collection then also allows writing explicit deformation families of Calabi–Yau hypersurfaces, and identifying their intersections with the  $\mathcal{S}_\alpha$ , to compute the corresponding “inherited” characteristics and so be of direct relevance to the ultimate goal of describing the Calabi–Yau hypersurfaces,  $\mathcal{X} \in F_m^{(n)}[c_1]$ .

For example, Hirzebruch’s original  $p_0(x, y) = x_0 y_0^m + x_1 y_1^m$  hypersurface [77] has its directrix identified as the zero locus of the following *equivalence class*(!) of sections:

$$\mathfrak{s}_0(x, y) := \left[ \left( \frac{x_0}{y_1^m} - \frac{x_1}{y_0^m} \right) + \lambda \frac{p_0(x, y)}{(y_0 y_1)^m} \right] = \begin{cases} +2x_0/y_1^m, & \lambda = +1, \text{ when } y_1 \neq 0, \\ -2x_1/y_0^m, & \lambda = -1, \text{ when } y_0 \neq 0. \end{cases} \quad (3.2)$$

The two  $\mathbb{P}_y^1$ -chartwise holomorphic local representatives specify a single section since<sup>14</sup>

$$\mathfrak{s}_0(x, y)|_{\lambda=+1} - \mathfrak{s}_0(x, y)|_{\lambda=-1} = 2 \frac{p_0(x, y)}{(y_0 y_1)^m} \stackrel{\text{id}}{=} 0, \quad \text{on } \{p_0(x, y) = 0\} =: F_m^{(n)}. \quad (3.3)$$

The directrix  $\mathfrak{s}_0(x, y)$  is holomorphic on  $F_m^{(n)} \subset \mathbb{P}^n \times \mathbb{P}^1$ , although not on  $\mathbb{P}^n \times \mathbb{P}^1$ . It is also transverse, since  $d\mathfrak{s}_0 = \left( \frac{dx_0}{y_1^m}, \frac{dx_1}{y_0^m}, \dots \right)$  cannot vanish anywhere over  $\mathbb{P}_y^1$ , so its zero locus in  $F_m^{(n)}$  is irreducible and smooth. Calabi–Yau hypersurfaces in  $F_m^{(n)}$  must have bi-degree  $(n, 2-m)$  in  $\mathbb{P}_x^n \times \mathbb{P}_y^1$ , and one finds that

$$f_0(x, y) \in \left( \bigoplus_{k=0}^2 (\phi_k(x) y_0^{2-k} y_1^k) \right) \mathfrak{s}_0(x, y), \quad \deg_{\mathbb{P}^n}[\phi_k(x)] = n-1, \quad (3.4)$$

indeed provide the full complement of regular anticanonical sections for  $m \geq 3$  when  $c_1(F_m^{(n)})$  is negative over the base- $\mathbb{P}_y^1$ , and provide the “missing” sections for the marginal case when  $c_1(F_2^{(n)})$  is null over the base- $\mathbb{P}_y^1$  [54]. For  $m=0, 1$ , there is no meaningful distinction between (3.4) and standard  $\text{deg}-(n, 2-m)$   $(x, y)$ -polynomials.

**Toric Translation:** Consider now the simple change of variables:

$$(x_0, x_1, \dots, x_n; y_0, y_1) \in \mathbb{P}^n \times \mathbb{P}^1 \quad (3.5a)$$

$$\rightarrow (p_\epsilon(x, y), \mathfrak{s}_0(x, y) = X_1, \{x_i = X_i\}_{i=2, \dots, n}, \{y_j = X_{n+j+1}\}_{j=0, 1}) \xrightarrow{p_\epsilon(x, y)=0} F_m^{(n)}. \quad (3.5b)$$

The Jacobian of the variable change being a constant, this (QFT-standard field redefinition) provides a 1–1 “direct translation” from the bi-projective embedding (3.1) to the toric definition (2.2), where the  $U(1; \mathbb{C})^2$ -charges  $q_1, q_2$  in (2.4) are indeed directly inherited from the  $\mathbb{P}^n \times \mathbb{P}^1$  homogeneity degrees.

This “direct translation” extends throughout the  $\epsilon_{i\ell}$ -deformation family (3.1) [56]: In hypersurfaces  $F_{m;\epsilon}^{(n)}$  (3.1) with more than one directrix, the biprojective-to-toric variable change (3.5) replaces the  $\mathbb{P}_{\beta x}^n$ -coordinates with directrices, in order and by increasing  $\mathbb{P}_y^1$  degree, while verifying that:

<sup>13</sup>In this context,  $\mathfrak{s}_\alpha(x, y)$  (defining  $\mathcal{S}_\alpha$ ) is “algebraically independent” from  $\mathfrak{s}_\beta(x, y), \mathfrak{s}_\gamma(x, y)$  means that there exists no algebraic relationship of the form  $\mathfrak{s}_\alpha(x, y) = y_0^{b_0} y_1^{b_1} \mathfrak{s}_\beta(x, y) + y_0^{c_0} y_1^{c_1} \mathfrak{s}_\gamma(x, y)$ .

<sup>14</sup>Viewed this way, the mechanism (3.2)–(3.3) insuring that  $\mathfrak{s}_0(x, y)$  is in fact a holomorphic section is *precisely* the same that enables the Wu–Yang construction of a magnetic monopole [97], and so turns out to be completely standard in QFT!

1. all directrices found as in Ref. [56, Construction 2.1] are transverse, so each of their zero-locus is an irreducible divisor;
2. the Jacobian of the variable change is constant;
3. the (3.4)-like linear combination of the directrices provides the full complement of regular anticanonical sections on  $F_{m;\epsilon}^{(n)}$ .

To showcase the so-constructed family and adapting from Ref. [59], consider the  $(n, m) = (3, 5)$  case of (3.1), several relevant members of which are provided in Table 2.<sup>15</sup> Differently deformed biprojective

**Table 2:** Several particular Hirzebruch scrolls within the  $(n, m) = (3, 5)$  deformation family (3.1)

deg.	biprojective defining section	name, GLSM charges
	$p_0(x, y) = x_0 y_0^5 + x_1 y_1^5$	$F_5^{(3)}$
$(-\frac{1}{5})$	$\mathfrak{s}_0(x, y) = \left[ \left( \frac{x_0}{y_1^5} - \frac{x_1}{y_0^5} \right) / p_0(x, y) \right]$	$\begin{array}{ccccc} X_1 & X_2 & X_3 & X_4 & X_5 \\ \hline 1 & 1 & 1 & 0 & 0 \\ -5 & 0 & 0 & 1 & 1 \end{array}$
	$p_1(x, y) = p_0(x, y) + x_2 y_0^4 y_1$	$F_{4,1}^{(3)}$
$(-\frac{1}{2})$	$\mathfrak{s}_{1a}(x, y) = \left[ \left( \frac{x_0 y_0}{y_1^5} - \frac{x_1}{y_0^4} + \frac{x_2}{y_1^4} \right) / p_1(x, y) \right]$	$\begin{array}{ccccc} X_1 & X_2 & X_3 & X_4 & X_5 \\ \hline 1 & 1 & 1 & 0 & 0 \\ -4 & -1 & 0 & 1 & 1 \end{array}$
$(-\frac{1}{2})$	$\mathfrak{s}_{1b}(x, y) = \left[ \left( \frac{x_0}{y_1} - \frac{x_1 y_1^4}{y_0^5} - \frac{x_2}{y_0} \right) / p_1(x, y) \right]$	
	$p_2(x, y) = p_0(x, y) + x_2 y_0^3 y_1^2$	$F_{3,2}^{(3)}$
$(-\frac{1}{3})$	$\mathfrak{s}_{2a}(x, y) = \left[ \left( \frac{x_0 y_0^2}{y_1^5} - \frac{x_1}{y_0^3} + \frac{x_2 y_0}{y_1^4} + \frac{x_3}{y_1^3} \right) / p_2(x, y) \right]$	$\begin{array}{ccccc} X_1 & X_2 & X_3 & X_4 & X_5 \\ \hline 1 & 1 & 1 & 0 & 0 \\ -3 & -2 & 0 & 1 & 1 \end{array}$
$(-\frac{1}{3})$	$\mathfrak{s}_{2b}(x, y) = \left[ \left( \frac{x_0}{y_1^2} - \frac{x_1 y_1^3}{y_0^5} - \frac{x_2}{y_0^2} \right) / p_2(x, y) \right]$	
	$p_3(x, y) = p_0(x, y) + x_2 y_0^4 y_1 + x_3 y_0^1 y_1^4$	$F_{3,1,1a}^{(3)} \approx_{\mathbb{R}} F_2^{(3)}$
$(-\frac{1}{3})$	$\mathfrak{s}_{3a}(x, y) = \left[ \left( \frac{x_0 y_0}{y_1^4} - \frac{x_1 y_1}{y_0^4} + \frac{x_2}{y_1^3} - \frac{x_3}{y_0^3} \right) / p_3(x, y) \right]$	$\begin{array}{ccccc} X_1 & X_2 & X_3 & X_4 & X_5 \\ \hline 1 & 1 & 1 & 0 & 0 \\ -3 & -1 & -1 & 1 & 1 \end{array}$
$(-\frac{1}{3})$	$\mathfrak{s}_{3b}(x, y) = \left[ \left( \frac{x_0}{y_1} - \frac{x_1 y_1^4}{y_0^5} - \frac{x_2}{y_0} - \frac{x_3 y_1^3}{y_0^4} \right) / p_3(x, y) \right]$	
$(-\frac{1}{3})$	$\mathfrak{s}_{3c}(x, y) = \left[ \left( \frac{x_0 y_0^4}{y_1^5} - \frac{x_1}{y_0} + \frac{x_2 y_0^3}{y_1^4} + \frac{x_3}{y_1} \right) / p_3(x, y) \right]$	
	$p_4(x, y) = p_0(x, y) + x_2 y_0^4 y_1 + x_3 y_0^3 y_1^2$	$F_{3,1,1b}^{(3)} \approx_{\mathbb{R}} F_2^{(3)}$
$(-\frac{1}{3})$	$\mathfrak{s}_{4a}(x, y) = \left[ \left( \frac{x_0 y_0^2}{y_1^5} - \frac{x_1}{y_0^3} + \frac{x_2 y_0}{y_1^4} + \frac{x_3}{y_1^3} \right) / p_4(x, y) \right]$	$\begin{array}{ccccc} X_1 & X_2 & X_3 & X_4 & X_5 \\ \hline 1 & 1 & 1 & 0 & 0 \\ -3 & -1 & -1 & 1 & 1 \end{array}$
$(-\frac{1}{3})$	$\mathfrak{s}_{4b}(x, y) = \left[ \left( \frac{x_0}{y_1} - \frac{x_1 y_1^4}{y_0^5} - \frac{x_2}{y_0} - \frac{x_3 y_1}{y_0^2} \right) / p_4(x, y) \right]$	
$(-\frac{1}{3})$	$\mathfrak{s}_{4c}(x, y) = \left[ \left( \frac{x_0 y_0}{y_1^2} - \frac{x_1 y_1^3}{y_0^4} + \frac{x_2}{y_1} - \frac{x_3}{y_0} \right) / p_4(x, y) \right]$	equivalent to $p_3(x, y)$
	$p_5(x, y) = p_0(x, y) + x_2 y_0^3 y_1^2 + x_3 y_0^2 y_1^3$	$F_{2,2,1}^{(3)} \approx_{\mathbb{R}} F_{1,1}^{(3)}$
$(-\frac{1}{2})$	$\mathfrak{s}_{5a}(x, y) = \left[ \left( \frac{x_0}{y_1^2} - \frac{x_1 y_1^3}{y_0^5} - \frac{x_2}{y_0^2} - \frac{x_3 y_1}{y_0^3} \right) / p_5(x, y) \right]$	$\begin{array}{ccccc} X_1 & X_2 & X_3 & X_4 & X_5 \\ \hline 1 & 1 & 1 & 0 & 0 \\ -2 & -2 & -1 & 1 & 1 \end{array}$
$(-\frac{1}{2})$	$\mathfrak{s}_{5b}(x, y) = \left[ \left( \frac{x_0 y_0^3}{y_1^5} - \frac{x_1}{y_0^2} + \frac{x_2 y_0}{y_1^3} + \frac{x_3}{y_1^2} \right) / p_5(x, y) \right]$	
$(-\frac{1}{2})$	$\mathfrak{s}_{5c}(x, y) = \left[ \left( \frac{x_0 y_0^2}{y_1^3} - \frac{x_1 y_1^2}{y_0^3} + \frac{x_2}{y_1} - \frac{x_3}{y_0} \right) / p_5(x, y) \right]$	

hypersurface scrolls (3.1) may well result in the same toric specification. Indeed, the explicit deformation family is far from *effective*: All hypersurfaces along a ray generated by  $\mathbb{C}^*$ -scaling any particular choice of finite and nonzero  $\epsilon_{i\ell}$ 's in (3.1) ends up corresponding to the same toric specification, which are thereby

<sup>15</sup>This also corrects a few simple typos [56].

“infinitesimally near” the central scroll,  $\{p_0(x, y) = 0\}$ . Also, some of those  $\mathbb{C}^*$ -rays turn out to provide the same toric specification, such as the symmetric deformation,  $p_4(x, y)$ , and the asymmetric deformation,  $p_5(x, y)$ , in Table 2; both of these produce  $F_{3,1,1}^{(3)}$ , and we return to this equivalence below. In turn, experimenting for  $m < 10$  and hand-picked deformations, seems to suggest—but by no means prove—the following contention:

**Conjecture 3.1:** *The family (3.1) is **complete**, in that it contains all the “cousins” to the central scroll,  $F_m^{(3)}$ , identified by:*

1. *partitioning the  $m$ -twist into an  $n$ -tuple,  $\vec{m} = (m_1, m_2, \dots, m_n)$ , with  $m_k \geq 0$  and any particular but fixed “taxicab”-magnitude,  $|\vec{m}| = \sum_{k=1}^n m_k = m$ ,*
2. *which is tantamount to having “distributed” the  $\deg(-\frac{1}{m})$  directrix into several  $\deg(-\frac{1}{m_k})$  directrices with  $\sum_k m_k = m$ , for the  $m_k > 0$ .*

From this admittedly small sample, but knowing that all compact complex-algebraic toric varieties can be embedded in a (sufficiently large) projective space, one may—perhaps—expect:

**Conjecture 3.2:** *All compact, complex-algebraic toric varieties can be embedded as complete intersections of hypersurfaces in some product of projective spaces.*

If proven, the claim of Conjecture 3.2 would imply that all hypersurfaces in complex-algebraic toric varieties [23, 24] in fact are particular cases of complete intersections in products of projective spaces (CICYs) [98–100]! The latter collection has been recorded to contain Calabi–Yau 3-folds with Euler characteristic and Hodge numbers [99, 101] that are but a rather small subset of that data found among the hypersurfaces in toric varieties [23, 24]—but, the CICY data has only ever been calculated for the *generic* members in the deformation classes of CICYs, which would have to be extended *in two ways*;

1. by identifying all particular cases within each deformation class that give rise to *discretely distinct* complex manifolds [54]—akin to the differing deformations in Table 2,

and

2. by including “generalized CICYs,” where some hypersurfaces have negative degrees of homogeneity with respect to some of the ambient projective spaces (as does the directrix (3.2)) [54, 95, 96]. Here, the hypersurfaces with all non-negative degrees define the complete intersections in Conjecture 3.2, and these include non-weak-Fano algebraic varieties—exemplified by  $F_{\vec{m}}^{(n)}$  with  $|\vec{m}| \geq 3$ .

**Veronese Twist:** Table 2 also exhibits three instances of the  $F_m^{(n)} \approx_{\mathbb{R}} F_{m(\bmod n)}^{(n)}$  diffeomorphism [54],  $F_{3,1,1a}^{(3)} \approx_{\mathbb{R}} F_2^{(3)} \approx_{\mathbb{R}} F_{3,1,1b}^{(3)}$  and  $F_{2,2,1}^{(3)} \approx_{\mathbb{R}} F_{1,1}^{(3)}$ , which we now explore.

In all three instances, the biprojective construction implies the  $U(1; \mathbb{C})^2$ -charges for the GLSM as indicated in the rightmost column of Table 2. For the underlying worldsheet QFT, this indicated basis is fully equivalent to the basis using  $\tilde{q}_2 = q_2 + q_1$  instead of  $q_2$ :

$$\begin{array}{c}
 \begin{array}{c|ccccc}
 F_{3,1,1a}^{(3)} \sim F_{3,1,1b}^{(3)} & X_1 & X_2 & X_3 & X_4 & X_5 \\
 \hline
 q_1 & 1 & 1 & 1 & 0 & 0 \\
 q_2 & -3 & -1 & -1 & 1 & 1 \\
 \hline
 F_{2,2,1}^{(3)} & X_1 & X_2 & X_3 & X_4 & X_5 \\
 \hline
 q_1 & 1 & 1 & 1 & 0 & 0 \\
 q_2 & -2 & -2 & -1 & 1 & 1
 \end{array}
 & \xrightarrow{\tilde{q}_2 = q_2 + q_1} &
 \begin{array}{c|ccccc}
 F_2^{(3)} & X_1 & X_2 & X_3 & X_4 & X_5 \\
 \hline
 q_1 & 1 & 1 & 1 & 0 & 0 \\
 \tilde{q}_2 & -2 & 0 & 0 & 1 & 1 \\
 \hline
 F_{1,1}^{(3)} & X_1 & X_2 & X_3 & X_4 & X_5 \\
 \hline
 q_1 & 1 & 1 & 1 & 0 & 0 \\
 \tilde{q}_2 & -1 & -1 & 0 & 1 & 1
 \end{array}
 \end{array} \tag{3.6a}$$

$$\begin{array}{c}
 \begin{array}{c|ccccc}
 F_{3,1,1a}^{(3)} \sim F_{3,1,1b}^{(3)} & X_1 & X_2 & X_3 & X_4 & X_5 \\
 \hline
 q_1 & 1 & 1 & 1 & 0 & 0 \\
 q_2 & -3 & -1 & -1 & 1 & 1 \\
 \hline
 F_{2,2,1}^{(3)} & X_1 & X_2 & X_3 & X_4 & X_5 \\
 \hline
 q_1 & 1 & 1 & 1 & 0 & 0 \\
 q_2 & -2 & -2 & -1 & 1 & 1
 \end{array}
 & \xrightarrow{\tilde{q}_2 = q_2 + q_1} &
 \begin{array}{c|ccccc}
 F_{1,1}^{(3)} & X_1 & X_2 & X_3 & X_4 & X_5 \\
 \hline
 q_1 & 1 & 1 & 1 & 0 & 0 \\
 \tilde{q}_2 & -1 & -1 & 0 & 1 & 1
 \end{array}
 \end{array} \tag{3.6b}$$

The latter of these  $U(1; \mathbb{C})^2$ -charge assignments are straightforwardly identified as the less-twisted Hirzebruch scrolls on the right-hand side in (3.6).

The  $F_m^{(n)}$  and  $F_{m-n}^{(n)}$  scrolls are distinct complex manifolds although they are diffeomorphic to each other; that is, they are “the same real manifold,” endowed however with differing complex structures [54]. This exhibits the higher-dimensional generalization of the well-known *discrete (jumping)* deformation of the complex structure in the classic 2-dimensional Hirzebruch surfaces; for relevance to characterizing Calabi–Yau hypersurfaces, see Refs. [18, 102] and also [54].

Following Ref. [59], we identify the Veronese-twisted mapping:

$$(x_0y_0^3, x_1y_1^3, x_2y_0^2y_1, x_3y_0y_1^2; y_0, y_1) \xrightarrow{-\tau} (\xi_0, \xi_1, \xi_2, \xi_3; \eta_0, \eta_1); \quad (3.7a)$$

$$\left[ \begin{array}{c} \mathbb{P}^3 \\ \mathbb{P}^1 \parallel 1 \\ 5 \end{array} \right] \left\{ \begin{array}{l} x_0y_0^5 + x_1y_1^5 + x_2y_1y_0^4 + x_3y_1^4y_0 \xrightarrow{-\tau} (\xi_0 + \xi_2)\eta_0^2 + (\xi_1 + \xi_3)\eta_1^2; \\ x_0y_0^5 + x_1y_1^5 + x_2y_0^4y_1 + x_3y_0^3y_1^2 \xrightarrow{-\tau} (\xi_0 + \xi_2 + \xi_3)\eta_0^2 + \xi_1\eta_1^2; \\ x_0y_0^5 + x_1y_1^5 + x_2y_0^3y_1^2 + x_3y_0^2y_1^3 \xrightarrow{-\tau} \xi_0\eta_0^2 + \xi_1\eta_1^2 + (\xi_2 + \xi_3)\eta_0\eta_1; \end{array} \right\} \left[ \begin{array}{c} \mathbb{P}^3 \\ \mathbb{P}^1 \parallel 1 \\ 2 \end{array} \right] \quad (3.7b)$$

$$\left[ \begin{array}{c} \mathbb{P}^3 \\ \mathbb{P}^1 \parallel 1 \\ 5 \end{array} \right] \left\{ \begin{array}{l} x_0y_0^5 + x_1y_1^5 + x_2y_1y_0^4 + x_3y_1^4y_0 \xrightarrow{-\tau} (\xi_0 + \xi_2)\eta_0^2 + (\xi_1 + \xi_3)\eta_1^2; \\ x_0y_0^5 + x_1y_1^5 + x_2y_0^4y_1 + x_3y_0^3y_1^2 \xrightarrow{-\tau} (\xi_0 + \xi_2 + \xi_3)\eta_0^2 + \xi_1\eta_1^2; \\ x_0y_0^5 + x_1y_1^5 + x_2y_0^3y_1^2 + x_3y_0^2y_1^3 \xrightarrow{-\tau} \xi_0\eta_0^2 + \xi_1\eta_1^2 + (\xi_2 + \xi_3)\eta_0\eta_1; \end{array} \right\} \left[ \begin{array}{c} \mathbb{P}^3 \\ \mathbb{P}^1 \parallel 1 \\ 2 \end{array} \right] \quad (3.7c)$$

$$\left[ \begin{array}{c} \mathbb{P}^3 \\ \mathbb{P}^1 \parallel 1 \\ 5 \end{array} \right] \left\{ \begin{array}{l} x_0y_0^5 + x_1y_1^5 + x_2y_1y_0^4 + x_3y_1^4y_0 \xrightarrow{-\tau} (\xi_0 + \xi_2)\eta_0^2 + (\xi_1 + \xi_3)\eta_1^2; \\ x_0y_0^5 + x_1y_1^5 + x_2y_0^4y_1 + x_3y_0^3y_1^2 \xrightarrow{-\tau} (\xi_0 + \xi_2 + \xi_3)\eta_0^2 + \xi_1\eta_1^2; \\ x_0y_0^5 + x_1y_1^5 + x_2y_0^3y_1^2 + x_3y_0^2y_1^3 \xrightarrow{-\tau} \xi_0\eta_0^2 + \xi_1\eta_1^2 + (\xi_2 + \xi_3)\eta_0\eta_1; \end{array} \right\} \left[ \begin{array}{c} \mathbb{P}^3 \\ \mathbb{P}^1 \parallel 1 \\ 2 \end{array} \right] \quad (3.7d)$$

as an evident candidate for the  $F_5^{(3)} \approx_{\mathbb{R}} F_2^{(3)}$  diffeomorphism. The non-constant Jacobian of this variable change,  $\det \left[ \frac{\partial(\xi, \eta)}{\partial(x, y)} \right] = (y_0y_1)^6$ , indicates that it is ill defined at the poles of  $\mathbb{P}_y^1$  as a holomorphic mapping—which is as expected, since  $F_5^{(3)}$  and  $F_2^{(3)}$  are distinct complex manifolds. Aiming only for a *diffeomorphism*, Ref. [59] reminds that the mapping (3.7) can in fact be *smoothed*—non-holomorphically(!)—using partitions of unity (“bump functions”) localized to within a small neighborhood over each of the poles of  $\mathbb{P}_y^1$ .

In a perhaps surprising twist (pun intended), the Veronese-twisted mapping (3.7) however *can* be modified to a constant-Jacobian variant (which is thereby better-suited for purposes of QFT in general and GLSMs in particular):

$$(x_0y_0^3 + x_2y_0^2y_1, x_1y_1^3 + x_3y_0y_1^2, \frac{x_2}{y_0^3}, \frac{x_3}{y_1^3}; y_0, y_1) \xrightarrow{-\tau'} (\xi_0, \xi_1, \xi_2, \xi_3; \eta_0, \eta_1), \quad (3.8a)$$

$$x_0y_0^5 + x_1y_1^5 + x_2y_0^4y_1 + x_3y_0y_1^4 \xrightarrow{-\tau'} \xi_0\eta_0^2 + \xi_1\eta_1^2; \quad (3.8b)$$

$$(x_0y_0^3 + x_2y_0^2y_1, x_1y_1^3 + x_3y_0^3, \frac{x_2}{y_0^3}, \frac{x_3}{y_1^3}; y_0, y_1) \xrightarrow{-\tau''} (\xi_0, \xi_1, \xi_2, \xi_3; \eta_0, \eta_1), \quad (3.8c)$$

$$x_0y_0^5 + x_1y_1^5 + x_2y_0^4y_1 + x_3y_0^3y_1^2 \xrightarrow{-\tau''} \xi_0\eta_0^2 + \xi_1\eta_1^2; \quad (3.8d)$$

and

$$(x_0y_0^3 + x_2y_0y_1^2, x_1y_1^3 + x_3y_0^2y_1, \frac{x_2}{y_0^3}, \frac{x_3}{y_1^3}; y_0, y_1) \xrightarrow{-\tau'''} (\xi_0, \xi_1, \xi_2, \xi_3; \eta_0, \eta_1), \quad (3.8e)$$

$$x_0y_0^5 + x_1y_1^5 + x_2y_0^3y_1^2 + x_3y_0^2y_1^3 \xrightarrow{-\tau'''} \xi_0\eta_0^2 + \xi_1\eta_1^2; \quad (3.8f)$$

at the obvious price of now involving rational monomials in (3.8a), (3.8c) and (3.8e)—which should not surprise, since the inverse maps of both (3.7) and (3.8) already involve rational monomials. It is as if the zeros and poles of the Jacobian of (3.7) have been moved into a balancing act of the zeros and poles in the individual components of the rational map (3.8).

**Remark 3.1:** The  $U(1; \mathbb{C})^2$ -transformation (3.6) is neither a flip nor a flop [30], but corresponds to the diffeomorphism  $F_m^{(n)} \approx_{\mathbb{R}} F_{m-n}^{(n)}$ ,<sup>16</sup> with two coordinate-level realizations provided in (3.7) and (3.8). These maps are straightforward to specify in the biprojective realization of  $F_m^{(n)}$ , but their precise (a) local geometry (blow-up/down combination?) and (b) toric geometry interpretations remain to be determined. An

<sup>16</sup>The mapping (3.7) incorporates the Veronese mapping,  $\mathbb{P}_y^1 \ni (y_0, y_1) \rightarrow (y_0^n, y_0^{n-1}y_1, \dots, y_1^n) \in \mathbb{P}_y^n$ , to then twist  $F_m^{(n)}$  as a  $\mathbb{P}_x^n$ -fibration over  $\mathbb{P}_y^1$  into a  $\text{diag}[\mathbb{P}_y^n \times \mathbb{P}_x^n]$ -fibration over the same base. Thus, the degree of the twist-equivalence,  $m \pmod{\underline{n}}$ , is canonically fixed to be multiples of the dimension of the fiber- $\mathbb{P}^n$ .

analogous Veronese-like twisting of the Cox variables,  $\{X_1, X_2, X_3\}$ , by the  $\{X_4, X_5\}$  would have degree-2—which would not reproduce the  $q_2 \rightarrow \tilde{q}_2$  change (3.6). In turn, no linear twisting of  $\{X_1, X_2, X_3\}$  by the  $\{X_4, X_5\}$ , as suggested by (3.6), can be uniform over  $\{X_1, X_2, X_3\}$ .  $\blacksquare$

Similar constant-Jacobian (albeit rational) variable changes can be found throughout the  $\epsilon_{i\ell}$ -deformation family when the  $q_2(X_i)$  become all nonzero and of the form shown at the left hand side of the equations (3.6).

### 3.2 Toric Classification

Given the correlation between the  $U(1; \mathbb{C})^2$ -charges and the generators of the toric fan, as detailed in Eqs. (2.3), (2.4) and the passage containing them, we can reconstruct the toric fans for the examples in Table 2. The generators of this fan being determined up to overall  $GL(3; \mathbb{Z})$  lattice redefinitions, it is gratifying to find that varying  $q_1, q_2$  as in Table 2,  $\nu_0, \dots, \nu_4$  in (2.4) may be held fixed, with only  $\nu_5$  having to vary; see Table 3. With this choice of  $\nu_5$  completing the definition of the fan  $\Sigma_{F_{5,\epsilon}^{(3)}}$ , the Mori vectors for this

**Table 3:** The various “cousins” of  $F_5^{(3)}$ , as defined by the biprojective embedding in  $A = \mathbb{P}^3 \times \mathbb{P}^1$ , which defines the  $q_a$ -charges, which then determine  $\nu_5$  for the toric realization, which in turn reduces  $q_2 \rightarrow \tilde{q}_2$ .

$F_{\vec{m}}^{(3)}$	$F_5^{(3)}$	$F_{4,1}^{(3)}$	$F_{3,2}^{(3)}$	$F_{3,1,1a}^{(3)}$	$F_{3,1,1b}^{(3)}$	$F_{2,2,1}^{(3)}$
$p_\epsilon(x, y) :$	$p_0(x, y)$	$\{p_1(x, y)$	$p_2(x, y)$	$p_3(x, y)$	$p_4(x, y)$	$p_5(x, y)$
$q_2 _A$	$(\bar{5}, 0, 0, 1, 1)$	$(\bar{4}, \bar{1}, 0, 1, 1)$	$(\bar{3}, \bar{2}, 0, 1, 1)$	$(\bar{3}, \bar{1}, \bar{1}, 1, 1)$	$(\bar{3}, \bar{1}, \bar{1}, 1, 1)$	$(\bar{2}, \bar{2}, \bar{1}, 1, 1)$
$\rightarrow \nu_5$	$\begin{pmatrix} -5 \\ -5 \\ 1 \end{pmatrix}$	$\begin{pmatrix} -3 \\ -4 \\ 1 \end{pmatrix}$	$\begin{pmatrix} -1 \\ -3 \\ 1 \end{pmatrix}$	$\begin{pmatrix} -2 \\ -2 \\ 1 \end{pmatrix}$	$\begin{pmatrix} -2 \\ -2 \\ 1 \end{pmatrix}$	$\begin{pmatrix} 0 \\ -1 \\ 1 \end{pmatrix}$
$q_2 _{\nu_5}$	$(\bar{5}, 0, 0, 1, 1)$	$(\bar{4}, \bar{1}, 0, 1, 1)$	$(\bar{3}, \bar{2}, 0, 1, 1)$	$(\bar{2}, 0, 0, 1, 1)$	$(\bar{2}, 0, 0, 1, 1)$	$(\bar{1}, \bar{1}, 0, 1, 1)$

For compactness in the  $q_2$  specification, “ $\bar{n}$ ” is used to denote “ $-n$ ”.

toric specification re-compute the  $q_a$ -charges of the  $U(1; \mathbb{C})^2$  gauge symmetry—and perfectly reproduce the overall (“taxicab”-magnitudes)  $m \rightarrow (m-n)$  twist reduction, as shown in the last-row entries in Table 3. This, of course, is consistent with this reduction being implemented by the  $GL(2 : \mathbb{Z})$  transformation,  $(q_1, \tilde{q}_2) = (q_1, q_2) \cdot \begin{pmatrix} 1 & 0 \\ 0 & 1 \end{pmatrix}$ .

The foregoing then implies that various choices of  $\nu_5$  characterize the distinct versions of the 5-twisted Hirzebruch 3-folds, resulting in the following generalization of (2.4):

$n = 3$	$\nu_0$	$\nu_1$	$\nu_2$	$\nu_3$	$\nu_4$	$\nu_5$
$\Sigma_{F_m^{(3)}} \left\{ \right.$	0	-1	1	0	0	$-m_1$
	0	-1	0	1	0	$-m_2$
	0	0	0	0	1	-1
	1	0	0	0	0	0
$q_1$	-3	1	1	1	0	0
$q_2$	$m_1 - 2(m_2 + 1)$	$m_2$	$m_2 - m_1$	0	1	1
$q_3$	$m_2 - 2(m_1 + 1)$	$m_1$	0	$m_1 - m_2$	1	1
$q_4$	$m_2 + m_1 - 2$	0	$-m_1$	$-m_2$	1	1
$q_5$	0	$m_2 + m_1 - 2$	$m_2 - 2(m_1 + 1)$	$m_1 - 2(m_2 + 1)$	3	3
<b>Cox variables:</b>	$X_0$	$X_1$	$X_2$	$X_3$	$X_4$	$X_5$

(3.9)

The increased list of possible choices of a basis of  $U(1; \mathbb{C})^2$ -charges exhibit a symmetry generated by the simultaneous swap  $(m_1 \leftrightarrow m_2, \nu_2 \leftrightarrow \nu_3, q_2 \leftrightarrow q_3)$ . Furthermore, whereas  $F_m^{(3)} := F_{-m, -m}^{(3)}$  holds by definition,  $F_{0,m}^{(3)}$  and  $F_{m,0}^{(3)}$  are isomorphic to them by virtue of the  $GL(3, \mathbb{Z})$ -equivalence of their respective fans:

- $(-m, -m, -1)$  coplanar with  $(0, 0, 1)$ ,  $(-1, -1, 0)$  in  $F_{-m, -m}^{(3)} =: F_m^{(3)}$ ,

2.  $(m, 0, -1)$  coplanar with  $(0, 0, 1), (1, 0, 0)$  in  $F_{m,0}^{(3)} \simeq F_m^{(3)}$ ,
3.  $(0, m, -1)$  coplanar with  $(0, 0, 1), (0, 1, 0)$  in  $F_{0,m}^{(3)} \simeq F_m^{(3)}$ .

The relating  $GL(3, \mathbb{Z})$ -transformation is the same that in the fiber plane  $(\nu_1, \nu_2, \nu_3)$  permutes the three vertices of the sub-fan of the fiber- $\mathbb{P}^2$ , providing a triality of descriptions.

The effects of such equivalences are easiest visualized and traced by plotting the  $(\hat{e}_1, \hat{e}_2)$ -plane in the  $N$ -lattice in a  $120^\circ$ -oblique coordinate system: cyclic  $GL(3; \mathbb{Z})$ -permutations of the fiber- $\mathbb{P}^2$  show as  $120^\circ$ -rotations. Accompanied by the reflections across  $\nu_1, \nu_2, \nu_3$  reflection, these generate the dihedral symmetry group  $D_3$  acting along the  $(\hat{e}_1, \hat{e}_2)$ -plane in the  $N$ -lattice. This induces a corresponding  $D_3$ -action in the  $\vec{m} := (m_1, m_2)$ -space, so that  $F_{\vec{m}}^{(3)} \approx F_{\vec{m}'}^{(3)}$  with  $\vec{m}' = \mathbb{D} \cdot \vec{m}$ , where  $\mathbb{D}$  is an element of the dihedral group,  $D_3$ , acting as the *mapping class group*. This permits limiting the  $(m_1, m_2)$ -range, e.g., to

$$\{ F_{m_1, m_2}^{(3)} : 0 \leq m_1 \leq m_1 \}, \quad \text{where} \quad F_{m,0}^{(3)} \stackrel{\text{def}}{=} F_m^{(3)}, \quad \text{and} \quad F_{m,m}^{(3)} = F_{-m}^{(3)}. \quad (3.10)$$

This specifies a fundamental domain of  $\mathbb{Z}^2/D_3$  in the  $(m_1, m_2)$ -plane:

This shows the starting corner of the dihedral-equivalent range  $0 \leq m_2 \leq m_1$  for convenience. The remainder of the  $(m_1, m_2)$ -plane is populated by the dihedral group action:  $R_3$  reflects this (3.11)-displayed upper-right  $60^\circ$ -wedge to the upward vertical  $60^\circ$ -wedge, and the two are then jointly  $120^\circ$ -rotated CCW, and once more to fill the plane.

### 3.3 The Anticanonical System

With the  $U(1; \mathbb{C})^2$ -charges for any given GLSM, such as presented in Table 2, one can address the choice of appropriate superpotentials, following the template in item 4, discussing the key requirement (1.4), and reorganizing the deformation-theoretic development in Ref. [59, §2].

We start with the anticanonical monomials of the  $p_0(x, y)$ -defined, “standard” Hirzebruch scroll,  $F_m^{(3)}$ , and then specialize to  $m = 5$  to discuss its variants in Table 2.

The multiply motivated (see Remark 1.1) key condition (1.4) always has an obvious solution, the so-called “fundamental monomial” [103],  $\Pi X := \prod_i X_i$ , so that the “defining function,”  $f(X)$ , in the superpotential,  $X_0 f(X)$ , may be regarded as a deformation of  $\Pi X$ . This, simplest of all  $F_m^{(3)}[c_1]$  superpotentials,  $W(X) = X_0 X_1 X_2 X_3 X_4 X_5$ , produces the  $F$ -term in (1.5) that is combinatorially and geometrically very simple, being the union of  $X_i$ -hyperplanes,  $\bigcup_i \{X_i = 0\} \subset F_m^{(n)}$  (in full generality). However, this space is also singular, and already in codimension-1, where two distinct hyperplanes intersect, which location is itself singular where three distinct hyperplanes intersect. In our 3-dimensional showcasing examples, this is where the hierarchy stops; in the physics-wise more interesting 4-dimensional case there is one more stratum of singularity in the so-obtained *polyhoron*. Since multiple intersections are restricted by the Stanley-Reisner ideal [30]—which for  $F_m^{(n)}$  (in full generality) differs from that of  $\mathbb{P}^n$ , this is not the literal but the conceptual analogue of the familiar regular pentahoron at infinity of so-called Dwork pencil of  $\mathbb{P}^4[5]$  hypersurfaces [104]; for relevance to string theory, see [105–107].

Whereas standard non-renormalization properties of worldsheet  $(2, 2)$ -supersymmetric GLSMs protect the superpotential from being changed by renormalization, we seek to *smooth* the zero-locus of its  $F$ -term, by following the standard practice in QFT: We *deform*  $\Pi X$  in  $W(X) = X_0 \Pi X$ , by replacing each  $X_i$  in  $\Pi X$  and in turn, with a monomial,  $m_i(X)$ , independent of  $X_i$  but such that  $q_a(m_i(X)) = q_a(X_i)$ . Formally, these replacements are implemented by the action of the operators  $\delta_i \stackrel{\text{def}}{=} m_i(X) \partial_i$  (no sum on  $i$ ). From the QFT side, the independence of  $m_i(X)$  from  $X_i$  is motivated by analogy with the requirement in quantum mechanics perturbation theory, where changes of any state,  $|*\rangle$ , must be orthogonal to  $|*\rangle$  itself, so as to preserve the norm and unitarity. From the algebraic geometry side, such replacements are generators of nontrivial  $U(1; \mathbb{C})^2$ -equivariant coordinate reparametrizations, also cited as (Demazure) “automorphisms stemming from roots” (here, the  $X_i$ ) [31, p. 48].<sup>17</sup>

Given the simple form of the starting point,  $\Pi X$ , the following observations follow:

1. The 1st order deformations are all of the form  $\delta_i \Pi X = m_i(X) (\partial_i \Pi X)$ , with no summation on  $i$ .
2. Since both  $(\partial_i \Pi X)$  and  $m_i(X)$  are  $X_i$ -independent, so is the collection  $\delta_i \Pi X$ .
3. Two distinct collections,  $\delta_i \Pi X$  and  $\delta_j \Pi X$ , have in common the subset of monomials that are independent of *both*  $X_i$  and  $X_j$ .
4. Three distinct collections have in common their subset of monomials that are independent of three of  $X_i, X_j, X_k$ 's, etc.
5. Each collection is delimited (bounded) by the monomials it has in common with another collection; write  $[\delta_i \Pi X]$  for the so-delimited collection.
6. Since  $\partial_i^2 \Pi X \equiv 0$ , there are no 2nd order deformations.

The union of these collections with the fundamental monomial,

$$(\Pi X) \cup \bigcup_i [\delta_i \Pi X] \quad (3.12)$$

has, astoundingly, an overall combinatorial structure that is well-nigh identical to the zero locus of  $\Pi X$  itself, the polyhoron mentioned above!

In this 3-dimensional lattice of monomials with the requisite charge (1.4), each  $X_i$ -independent subset forms a “pane,” each  $X_i, X_j$ -independent subset forms a “line” common to the  $X_i$ - and  $X_j$ -“pane,” and each  $X_i, X_j, X_k$ -independent subset is a corner which is common to those three “panes.” In turn, each “planar” subset of monomials is delimited by the monomials that it has in common with another “planar” subset, and so on.<sup>18</sup> This structure is generated by the  $X_i$ -replacement operators,  $\delta_i$ , which are as follows:

$i:$	$m_i(X)$	$\mapsto$	$\delta_i \Pi X$	
1:	$X_2^{\ell-1} X_3^{2-\ell} X_4^{r-1} X_5^{1-m-r}$	$\mapsto$	$X_2^\ell X_3^{3-\ell} X_4^r X_5^{2-m-r}$	(3.13)
2 or 3:	$X_1^{k-1} X_{3 2}^{2-k} X_4^{r-1} X_5^{1+(k-1)m-r}$	$\mapsto$	$X_1^k X_{3 2}^{3-k} X_4^r X_5^{2+(k-1)m-r}$	
4 or 5:	$X_1^{k-1} X_2^{\ell-1} X_3^{2-k-\ell} X_{5 4}^{1+(k-1)m}$	$\mapsto$	$X_1^k X_2^\ell X_3^{3-k-\ell} X_{5 4}^{2+(k-1)m}$	

where linear combinations over varying  $k, \ell, r$  are understood.

Two “planar” subsets have in common the monomials found by seeking the condition that makes the  $\delta_i \Pi X$ -monomials also  $X_j$ -independent. For example,

$$[\delta_1 \Pi X] \cap [\delta_2 \Pi X] = \left[ \widehat{X}_2^\ell X_3^{3-\ell} X_4^r X_5^{2-m-r} \right]_{\ell=0} = X_3^3 X_4^r X_5^{2-m-r}; \quad (3.14)$$

<sup>17</sup>Each such automorphism is generated by a relation of the form  $X_i - \lambda m_i(X) \sim 0$ , effectively substituting  $X_i$  by a multiple of  $m_i(X)$ —which is *precisely* how the  $m_i(X) \partial_i$  act.

<sup>18</sup>This in particular implies that any non-lattice (“fractional”) intersections of such lattice “panes” do not in fact delimit any of the combinatorial strata of the poset.



subsequent discussion to the Corollary 3.1 and Remark 3.2, with the Newton *multitope*,<sup>19</sup>  $\Delta_{F_5^{(3)}}$ , and the *multifan* [64–75] it is defined to span [55–57].

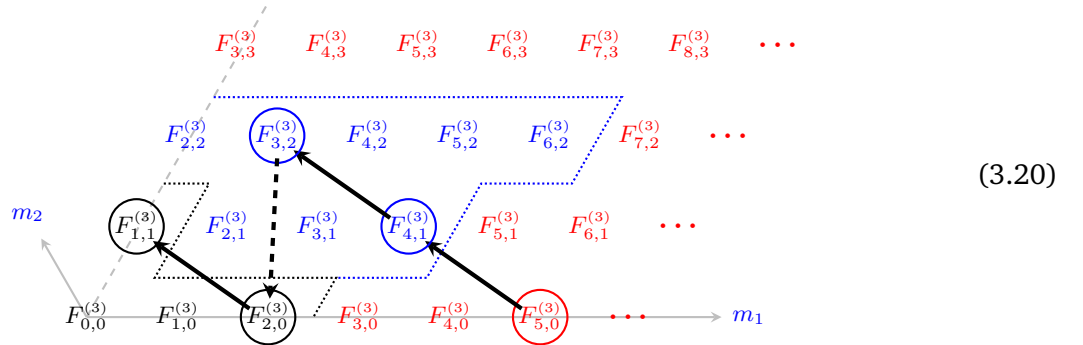
In turn and as presented in Ref. [59], each generator  $\delta_i \propto \partial_i$  by definition acts transversally to the  $X_i$ -independent “pane” of anticanonical monomials, so that the collection  $\{\delta_i\}$  spans the face-wise polar, i.e., *transpolar*<sup>20</sup> multitope,  $\Delta_{F_5^{(3)}}^* = (\Delta_{F_5^{(3)}})^\nabla$  and the multifan it spans,  $\Sigma_{F_5^{(3)}} \in \Delta_{F_5^{(3)}}^*$ —again all in perfect agreement with Refs. [55–57]. In particular, the poset automatically includes the monomials that are rational for  $m \geq 3$ :

$$\oplus_{\ell,r} X_2^\ell X_3^{3-\ell} X_4^r X_5^{2-m-r} = \begin{cases} (X_2 \oplus X_3)^3 (X_4 \oplus X_5)^{2-m}, & \text{for } m \leq 2; \\ (X_2 \oplus X_3)^3 \left(\frac{1}{X_4} \oplus \frac{1}{X_5}\right)^{m-2}, & \text{for } m \geq 3. \end{cases} \quad (3.19)$$

They are omitted in the complex-algebraic standard toric geometry, but are germane to smoothing the Tyurin-degenerate Calabi–Yau hypersurfaces in  $F_m^{(n)}$ , which are for  $m \geq 3$  standardly deemed “unsmoothable” [56]. As the smoothing deformation-motivated construction (3.12)–(3.19) and especially the poset in Figure 3 imply, the inclusion of precisely these rational monomials fits well within the GLSM framework; see also [56, § 4].

**Deformations of  $F_5^{(3)}$ :** We now turn to the deformations of  $F_5^{(3)}$ , as listed in Table 2, forgoing however the detailed analysis and argumentation as done above for  $F_5^{(3)}$ , and presenting instead the corresponding Newton and spanning multitopes,  $\Delta_{F_m^{(3)}}$  and  $\Delta_{F_m^{(3)}}^*$ ; see Figure 4. This makes manifest the overall combinatorial structure of the collection anticanonical monomials (3.12) for each Hirzebruch scroll,  $F_m^{(3)}$ . Generally in the  $\Delta_{F_m^{(3)}}$ -plots in Figure 4, the power of  $X_1$  drop from 3 in the back to 0 in the front; the powers of  $X_2, X_3$  “trade” left–right, and the powers of  $X_4, X_5$  “trade” up–down. In the (smaller) spanning polytopes, concave edges are (red) highlighted and are the transpolar images of the “extensions” in the Newton multitopes, comprising the frontmost “hanging” segments (red points). The spanning polytope  $\Delta_{F_{3,1,1}^{(3)}}^* \approx_{\mathbb{R}} \Delta_{F_2^{(3)}}^*$  exceptionally has a lattice point along its (upper back, slanted) edge, which is the transpolar image of the frontmost edge in  $\Delta_{F_{3,1,1}^{(3)}} \approx_{\mathbb{R}} \Delta_{F_2^{(3)}}$ , which in turn may be seen (progressing from left to right in Figure 4) as the result of the collapsed “extension.”

The deformation sequence in Table 2 and Figure 4 may thus also be identified in the plot of scrolls (3.11):



<sup>19</sup>This Latin/Greek heterotic portmanteau of (possibly) multi-layered+polytope” denotes a real  $n$ -dimensional polyhedral complex of finitely many convex  $n$ -dimensional polytopes,  $\Delta := \sqcup_{\alpha} \Delta_{\alpha}$ , which contains each face of each  $\Delta_{\alpha}$ ,  $\Delta_{\alpha} \cap \Delta_{\beta}$  is a face of both, and  $\Delta$  is a poset, such as in Figure 3. Moreover, each  $\Delta_{\alpha}$  has lattice- $\Lambda$ -primitive vertices and the complex is homeomorphic to an  $n$ -ball [108], although  $\Delta$  need only immerse in  $\mathbb{R}^n \supset \Lambda$ . Thus, polytopes are multitopes that do embed in  $\mathbb{R}^n$ ; their image in  $\mathbb{R}^n$  does not self-cross.

<sup>20</sup>The *transpolar operation* is the face-wise *polar operation* [27–30] applied iteratively throughout the poset of a multitope, and subject to the universal inclusion-reversing nature of the polar operation [55–57]; on convex polytopes, it is identically the same as the standard polar operation.

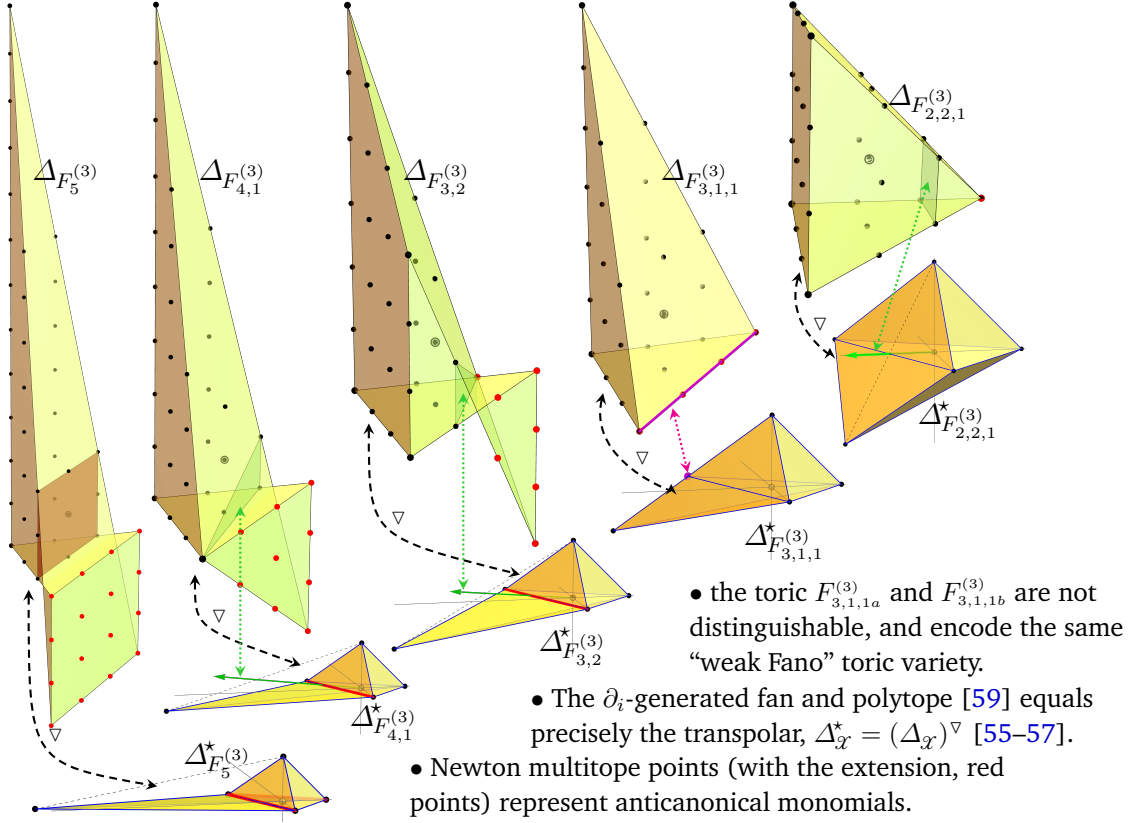


**Figure 4:** The progression of Newton and spanning multitope for the deformations in Table 2. The two multitope are related by the involutive *transpolar* ( $\nabla$ ) operation [55–57]. Truncating the Newton multitope to a convex polytope at the drawn-in (green-shaded) facet encodes a blowup of that  $F_m^{(3)}$ , indicated by the new vertex-arrow in the spanning polytope; see text. The (magenta-highlighted) lower-right edge in  $\Delta_{F_{3,1,1}^{(3)}}$  may be seen as the collapsed lower-right rectangle in  $\Delta_{F_5^{(3)}}$ .

which jointly help explaining the key differences between the models along this deformation path, as well as the partitioning of the starting corner of this (wedge-shaped)  $D_3$ -primitive domain in the space of all  $F_m^{(3)}$  Hirzebruch scrolls, and then also their Calabi–Yau hypersurfaces:

$F_5^{(3)}$ : This initial scroll has a (complete, extended) Newton multitope with its “extension” presented as the frontmost  $3 \times 3$  pane of (red) points. While all other points represent *regular* (non-negative  $X_i$ -powers) anticanonical monomials, the (red) “extension” points represent rational monomials,  $(X_2 \oplus X_3)^3 \left( \frac{1}{X_4} \oplus \frac{1}{X_5} \right)^3$ , listed in the bottommost “pane” in the poset Figure 3; see (3.19). As indicated by the darker shaded vertical  $2 \times 2$  square centered at the origin, there is no way to trim away the extension of  $\Delta_{F_5^{(3)}}$  without exposing the origin into a facet, i.e., the entire “regular” part of the Newton polytope occupies only a half-space (the back, as depicted in Figure 4, leftmost). Thereby, no *regular* anticanonical  $X_i$ -polynomial can be transverse, all Calabi–Yau hypersurfaces are Tyurin degenerate and standardly deemed “unsmoothable”—but are readily smoothed by including the “extension” rational monomials [55, 56].

$F_{4,1}^{(3)}$ : The situation improves already with the first deformation: The  $\Delta_{F_{4,1}^{(3)}}$  Newton multitope, second from left in Figure 4, *can* be trimmed at the (green) shaded 3-point triangle, and so trim away the nine “extension” (red point) monomials. The remaining convex polytope still encloses the origin, so that generic anticanonical (regular) polynomials are transverse, and define smooth Calabi–Yau hypersurfaces with *no need* to include the nine rational monomials.

In turn, the so-reduced Newton polytope also corresponds to another, related underlying ambient space, encoded by the introduction of the new facet (the 3-point triangular “pane”), which has its own normal,

$$\left[ \begin{pmatrix} 2 \\ -1 \\ -1 \end{pmatrix}, \begin{pmatrix} -1 \\ -1 \\ -1 \end{pmatrix}, \begin{pmatrix} -1 \\ 1 \\ 0 \end{pmatrix} \right] \xleftrightarrow{\nabla} \begin{pmatrix} -2 \\ -3 \\ 0 \end{pmatrix} = \nu_6 \leftrightarrow \partial_6, \quad (3.21)$$

and which introduces a new vertex. The original  $\nu_1$  turns out to be in the relative interior of the new  $[\nu_3, \nu_5, \nu_6, \nu_4]$  facet, and the polytope spanned by  $\{\nu_2, \nu_3, \nu_4, \nu_5, \nu_6\}$  is convex (reflexive,<sup>21</sup> moreover), and encodes  $\text{Bl}[F_{4,1}^{(3)}]$ , a blowup of  $F_{4,1}^{(3)}$ . This introduces a new  $(1, 1)$ -form, which is then inherited by the Calabi–Yau hypersurface, which in turn is thus substantially changed.

$F_{3,2}^{(3)}$ : This deformation of  $F_5^{(3)}$  is qualitatively similar to  $F_{4,1}^{(3)}$ , in that the Newton multotope also can be trimmed at the (green) shaded 3-point triangle, and so trim away the six “extension” (red point) monomials. This leaves a convex polytope that still encloses the origin, so that generic anticanonical (regular) polynomials are transverse, and define smooth Calabi–Yau hypersurfaces with *no need to include* the six rational monomials. The so-reduced Newton polytope again also corresponds to a blowup of  $F_{3,2}^{(3)}$ , which again substantially changes the Calabi–Yau hypersurfaces.

$F_{3,1,1}^{(3)} \approx_{\mathbb{R}} F_2^{(3)}$ : This deformation is diffeomorphic to the marginal, “weak Fano”  $F_2^{(3)}$ , with a strongly convex Newton polytope. This equivalence appears to be realized by a simple change of the  $U(1; \mathbb{C})^2$ -charge basis (3.6a), and so seems to be a straightforward equivalence relation between the corresponding GLSMs. This is further supported by the explicit coordinate-level mapping (3.7) and its constant-Jacobian variant (3.8). Both  $\Delta_{F_2^{(3)}}$  and  $\Delta_{F_2^{(3)}}^*$  are convex and reflexive, and each other’s polars [48].

$F_{2,2,1}^{(3)} \approx_{\mathbb{R}} F_{1,1}^{(3)}$ : This final deformation is diffeomorphic, and related by (3.6a), (3.7) and (3.8) to the scroll of the same overall  $m = 2$  twist, but which has two distinct  $\deg(-\frac{1}{2})$  directrices instead of a single of  $\deg(-\frac{1}{2})$ . Now both the Newton and the spanning polytopes are strongly convex, reflexive, and each other’s polars [48].

These cases exemplify the characteristics of all Hirzebruch scrolls in the map (3.20), which may then be summarized as follows:

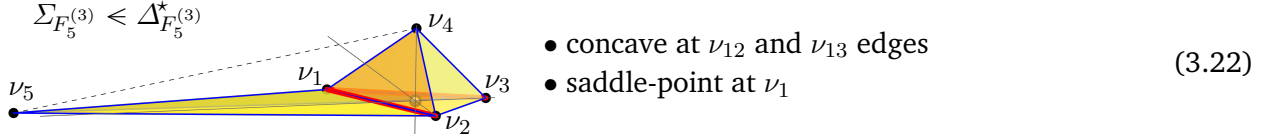
**Corollary 3.2:** *Modulo the  $D_3$ -action, the  $\vec{m}$ -plane of Hirzebruch 3-folds  $F_{\vec{m}}^{(3)}$  contains three classes:*

1. *The four 3-folds,  $F_{0,0}^{(3)} \stackrel{\text{def}}{=} F_0^{(3)}$ ,  $F_{1,0}^{(3)} \stackrel{\text{def}}{=} F_1^{(3)}$ ,  $F_{2,0}^{(3)} \stackrel{\text{def}}{=} F_2^{(3)}$  and  $F_{1,1}^{(3)} \stackrel{\text{def}}{=} F_{-1}^{(3)}$  have convex, in fact reflexive, spanning and Newton polytopes that are each other’s polars.*
2. *The remaining infinite collection of 3-folds all have non-convex but VEX spanning and Newton polytopes [55–57]. These however belong to two classes:*
  - (a) *The convex integral hull of the standard part of the Newton polytopes of the eight special 3-folds,  $F_{2,1}^{(3)}$ ,  $F_{3,1}^{(3)}$ ,  $F_{4,1}^{(3)}$ ,  $F_{2,2}^{(3)}$ ,  $F_{3,2}^{(3)}$ ,  $F_{4,2}^{(3)}$ ,  $F_{5,2}^{(3)}$  and  $F_{6,2}^{(3)}$  **does** enclose the origin.*
  - (b) *The convex integral hull of the standard part of the Newton polytopes of the remaining infinitely many 3-folds **do not** enclose the origin; the extension must be included to that end. The first few in this infinite class are indicated in (3.20) by red ink.*
3. *The same explicit deformation family (3.1) contains all Hirzebruch scrolls,  $F_{\vec{m}}^{(n)}$ , with “taxicab”-magnitudes  $|\vec{m}| = \sum_i m_i = m - kn$ , where  $k = 0, \dots, \lfloor \frac{m}{n} \rfloor$ .*

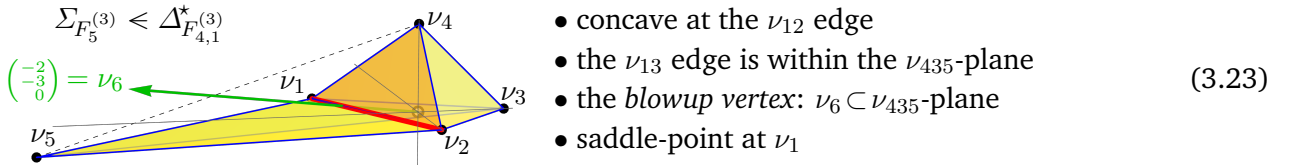
<sup>21</sup>That is, the *standard polar* operation [28–30] produces a lattice polytope and squares to the identity.

**Remark 3.3:** This classification/partitioning (3.9)–(3.11) and (3.20) readily generalizes to higher dimensions, and is based on the symmetries of the spanning polytope of fiber- $\mathbb{P}^{n-1}$ : viewed as an equilateral simplex, its symmetries are generated by reflections and rotations. In turn, for the original Hirzebruch (complex 2-dimensional) surfaces, this classification reduces to the well known fact that  $F_{-m}^{(2)} = F_m^{(2)}$ , and that  $m = 0, 1, 2, \dots$ . It is worth noting that overall, cases 1 in Corollary 3.2 are best studied and understood, cases 2a have room to explore, and cases 2b are the least studied, least understood—yet, the most abundant.  $\blacksquare$

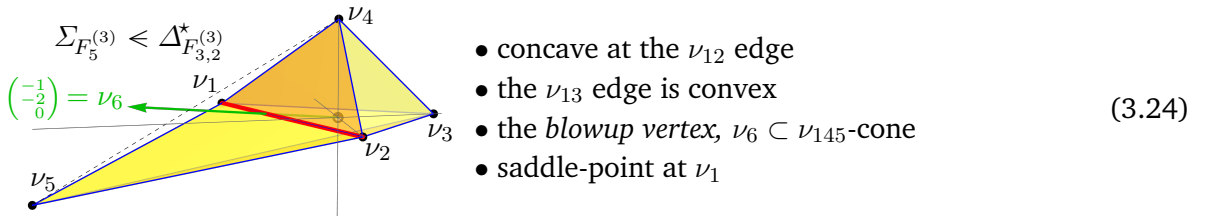
In turn, a closer look at the *fan-spanning polytopes*,  $\Delta_{F_{3,2}}^*(3)$ ,  $\Delta_{F_{4,1}}^*(3)$  and  $\Delta_{F_5}^*(3)$ , re-displayed here from Figure 4 in greater detail provides additional information:



The dotted  $\nu_{4,5}$  line indicates the edge from the *convex hull* of the vertices; indeed  $\Delta_{F_5}^*(3)$  may be regarded as obtained from this convex hull by “VEXing”: by trimming away the “non-star (not adjacent to the origin) simplices,”  $\nu_{1524}$  and  $\nu_{1435}$ —dubbed *divots* in Ref. [76]. Modifying a polytope by trimming away non-star simplices leaves a “star-triangulated” possibly non-convex (as here) VEX polytope [55–57]. In turn, the convex hull encodes the singular weighted projective space,  $\mathbb{P}_{(5:5:1:1)}^3$ .



The displayed configuration of this polytope was dubbed the *hammock* [57], as opposed to the *tent* configuration that includes the  $\nu_{1524}$ -simplex and corresponds to the singular weighted projective space,  $\mathbb{P}_{(1:1:3:4)}^3$ . The former is non-convex but VEX, while the latter is convex but not reflexive [48]: its standard polar,  $(\text{Conv}[\Delta_{\mathbb{P}_{(1:1:3:4)}^3}^*])^\circ$  has a fractional (non-lattice) vertex that would correspond to a radical monomial. Its desingularizing blowup coincides with the convex hull enclosing also a blowup vertex,  $\nu_6$ , that corresponds also to the blowup,  $\text{Bl}_{\nu_6}^\uparrow[F_{4,1}^{(3)}]$ , which is both convex and reflexive.



The displayed (hammock) polytope is non-convex but VEX, while the *tent* configuration (including the  $\nu_{1524}$ -simplex) is convex and reflexive and corresponds to the singular  $\mathbb{P}_{(1:1:1:3)}^3$ . The convex hull enclosing also  $\nu_6$  is also convex and reflexive, and corresponds to the blowup,  $\text{Bl}_{\nu_6}^\uparrow[F_{3,2}^{(3)}]$ .

— o —

This analysis firmly connects the entire deformation family of each biprojective embedding of Hirzebruch scrolls to the well-studied constructions in weighted projective spaces and (complex-algebraic) toric varieties—while grounded in their application within the underlying worldsheet QFT and GLSM structure,

relating this to toric geometry as needed—and extends them by including the non-Fano cases,  $F_m^{(n)}$  with  $m \geq 3$ . This indicates an apparently unbounded collection of ambient spaces,  $A = F_m^{(n)}$ , in which to embed the Calabi–Yau hypersurfaces of ultimate interest, and so may be seen as a vast generalization of Gross’ and Ruan’s *non-algebraic deformation equivalence* example,  $F_{(2,1,1,0)}^{(4)} \approx_{\mathbb{R}} F_0^{(4)}$  [109, 110].

Let us close with the following observations:

1. Trimming a 2-dimensional convex polygon by removing non-star simplices of a particular triangulation to obtain a star-triangulated non-convex (but VEX) polygon is by now called *VEXing*. This *reduction* of a polygon necessarily implies an *expansion* in its transpolar/dual polygon, by introducing at least one new vertex.
2. VEXing a 3-dimensional convex polytope need not introduce any new vertex in its transpolar/dual, as seen when trimming from the *tent* to the (displayed) *hammock* configurations in (3.23) and (3.24). The convex hull however is invariably found to be (see footnote 25) singular and requires some local *surgery* (typically, blowup) to desingularize the so-defined underlying toric space.
3. In four dimensions, one may analogously trim even *reflexive* polytopes, which was dubbed (lower-case styled) *vexing* [76, 111, 112], which also introduces codimension-2 (“pane”) non-convexity but now neither the original reflexive polytope nor its vexed non-convex retriangulation need be singular.<sup>22</sup> The so-obtained non-convex polytopes encode non-weak-Fano toric varieties and their Calabi–Yau hypersurfaces, which are combinatorially more abundant than the routinely studied (fine, regular and star-triangulated, “FRST”) convex and reflexive polytopes, and increasingly rapidly so: already by  $h^{1,1} \leq 7$ , the number of vex-triangulated (and so non-convex-trimmed) polytopes grows beyond twice as many as FRSTs [76]. Since the Kreuzer–Skarke database [23, 24] spans  $1 \leq h^{1,1} \leq 491$ , the likely very substantial preponderance of vex triangulations should be evident.

VEX (but still “ordinary,” “plain”) *polytopes* are more abundant yet, their convex hulls not being required to be reflexive. Furthermore, by including also self-crossing and otherwise multi-layered cases, the full complement of VEX *multitopes* (4-dimensional analogues of  $\Delta_{F_5^{(3)}}$ ,  $\Delta_{F_{4,1}^{(3)}}$  and  $\Delta_{F_{3,2}^{(3)}}$  in Figure 4, see also [57]) is vastly more plentiful.

## 4 Reflexions in the Mirror

As argued above, the entire explicit deformation family (3.1) of Calabi–Yau hypersurfaces in Hirzebruch scrolls may be realized within the GLSM framework [19, 20]—perhaps even more obviously so within the predecing framework of constrained (nonlinear gauged) sigma models [41, 42, 87–89]. As shown in Sections 3, this deformation family (3.1), as showcased in Table 2, contains several distinct Hirzebruch 3-folds exhibiting a hierarchy of five distinct types of combinatorial structures on display in Figure 4:

- A.  $F_{2,2,1}^{(3)}$ : both the Newton polytope  $\Delta_{F_{2,2,1}^{(3)}}^*$  and the spanning polytope  $\Delta_{F_{2,2,1}^{(3)}}^*$  are *reflexive*, moreover *strongly convex*; this is routine complex-algebraic toric geometry.
- B.  $F_{3,1,1}^{(3)}$ : both polytopes are reflexive; the Newton polytope  $\Delta_{F_{2,2,1}^{(3)}}^*$  is *strongly convex* and *reflexive*, but the spanning polytope  $\Delta_{F_{2,2,1}^{(3)}}^*$  is “only” convex: In this deformation, the vertex  $\nu_1$  “moved” into the  $\nu_{45}$ -line, now an edge of the fan-spanning polytope, which effectively encodes the ( $\mathbb{Z}_2$ -singular) weighted projective space  $\mathbb{P}_{(1:1:2:2)}^3$ .

<sup>22</sup>I thank Elijah Sheridan for verifying and informing me of this feature.

- C.  $F_{3,2}^{(3)}$ : the spanning polytope  $\Delta_{F_{3,2}}^{\star(3)}$  is *concave* at the  $\nu_{12}$  edge and its adjacent facets, and so cannot be reflexive. The Newton multitope  $\Delta_{F_{3,2}}^{\star(3)}$  is self-crossing flip-folded, but its regular part (without the extension rational monomials) suffices to provide transverse anticanonical sections. The “tent”-formed  $\text{Conv}[\Delta_{F_{3,2}}^{\star(3)}]$  is *reflexive*, its polar being a lattice Newton polytope, which is (of course) also *reflexive*.
- D.  $F_{4,1}^{(3)}$ : the spanning polytope  $\Delta_{F_{4,1}}^{\star(3)}$  is *concave* at the  $\nu_{12}$  edge and its adjacent facets. The Newton multitope  $\Delta_{F_{4,1}}^{\star(3)}$  is self-crossing flip-folded, but its regular part (without the extension rational monomials) suffices to provide transverse anticanonical sections. However,  $\text{Conv}[\Delta_{F_{4,1}}^{\star(3)}]$  is *not reflexive*: its polar Newton polytope has a *fractional vertex*.
- E.  $F_5^{(3)}$ : the spanning polytope  $\Delta_{F_5}^{\star(3)}$  is (saddle-point) non-convex at the  $\nu_1$  vertex, concave at the adjacent edges,  $\nu_{12}$  and  $\nu_{13}$ , and at their adjacent facets. The Newton multitope  $\Delta_{F_5}^{\star(3)}$  is self-crossing flip-folded, and now its extension *rational monomials are necessary* to provide transverse anticanonical sections. Also,  $\text{Conv}[\Delta_{F_5}^{\star(3)}]$  is *not reflexive*: its polar Newton polytope has *fractional vertices*.

The by now standard, routine construction of mirror models [48] is defined only for models of type A. and B., such as the *sufficiently generic* deformations within the family (3.1).

The explicitly continuous and even complex-algebraically describable deformations throughout this family then imply that mirror duality ought to extend throughout, also to the less generic deformations. To this end, Refs. [55–59] continue verifying a direct generalization of the “transposition mirror construction” [44] to the remaining (type C., D. and E.) specializing deformations within explicit deformation families such as (3.1)—as a showcasing template, indicating the need for a systematic and foundational study.

#### 4.1 Non-Convexity and Self-Crossing

**Non-Algebraic Aspects:** The fan-spanning polytopes,  $\Delta_{F_{\bar{m}}}^{\star(n)}$ , such as shown in Figure 4 are all (ordinary) polytopes, although several of them are non-convex.<sup>23</sup> Their transpolar Newton multitopes,  $\Delta_{F_{\bar{m}}}^{(n)} = (\Delta_{F_{\bar{m}}}^{\star(n)})^\nabla$ , such as shown in Figure 4, motivated directly from the smoothing deformations of the GLSM superpotential, include self-crossing polyhedral bodies,  $\Delta_{F_5}^{(3)}$ ,  $\Delta_{F_{4,1}}^{(3)}$  and  $\Delta_{F_{4,1}}^{(3)}$ . These clearly do not belong to the (standard) complex-algebraic toric geometry framework, but do turn up in studies of *symplectic*  $U(1)^r$ -equivariant geometry—which is fascinating, since mirror duality is indeed supposed to “swap” complex-algebraic and (special) symplectic geometry [51–53]!

In that symplectic geometry framing, self-crossing multitopes have been called *virtual polytopes* [113, 114], *twisted polytope* [115], and fit in the generalized notion dubbed *polyhedral complex* [108]. Now, each reflexive polytope admits star-triangulations, each of which spans a central fan consisting of cones subtended by the facets of the polytope. Analogously, VEX multitopes admit star-triangulations, each of which spans a central multifan of cones over its facets<sup>24</sup>—in the case of Newton multitopes,  $\Delta_{F_5}^{(3)}$ ,  $\Delta_{F_{4,1}}^{(3)}$  and  $\Delta_{F_{4,1}}^{(3)}$ , over the “panes” of monomials shown in Figure 3.

<sup>23</sup>Polytopes are multitopes that *embed* in  $\mathbb{R}^n$ , while more general multitopes only *immerse*, such as the three self-crossing flip-folded Newton multitopes (see footnote 19),  $\Delta(F_5^{(3)})$ ,  $\Delta(F_{4,1}^{(3)})$  and  $\Delta(F_{3,2}^{(3)})$ , in Figure 4. Note that (complex-algebraic) toric geometry focuses on convex polytopes [27–31], so practitioners tend to drop the “convex” qualifier for expediency; needless to say, *reflex* angles/cones and *non-convex* polygons and polytopes have not ceased to exist, and in fact do turn up even in complex-algebraic toric geometry: (3.22)–(3.24).

<sup>24</sup>“VEX multitopes” were defined [55–57] as polyhedral complexes that span complete multifans [64–67] and on which the transpolar.

**Mirror Mapping:** The key operation in the complex-algebraic toric geometry framing of mirror duality [48]—which applies perfectly to the “sufficiently generic” of the deformations (type A. and B., in the above listing)—is the swapping of the rôles of the spanning and the Newton polytope. As detailed in Refs. [57–59]:

1. Given a “well known” ambient toric variety,  $A$ , encoded by the fan that star-subdivides its spanning polytope,  $\Sigma_A \triangleleft \Delta_A^*$ ,
2. the lattice points,  $u_j \in \mathbb{Z}^n \cap \Delta_A$ , of its Newton polytope ( $\Delta_A = (\Delta_A^*)^\circ$ ) encode the sections of the anticanonical line bundle,  $\Gamma(\mathcal{K}_A^*) = \bigoplus_{u_j} a_j \prod_i x_i^{\langle \nu_i | u_j \rangle + 1}$ , in terms of the Cox variables,  $x_i \mapsto \nu_i \in \Sigma_A^{(1)} \xrightarrow{1-1} \Delta_A^{*(1)}$ , one for each vertex of  $\Delta_A^*$ .
3. The zero locus of a (transverse) section,  $f(x) \in \mathcal{K}_A^*$ , is a (smooth) Calabi–Yau hypersurface,  $\mathcal{X} := \{f(x)=0\} \subset A$ .
4. The mirror Calabi–Yau space,  $\tilde{\mathcal{X}}$ , is then the hypersurface  $\tilde{\mathcal{X}} := \{g(y)=0\} \subset B$ , where the toric variety  $B$  is defined by swapping the rôles of  $\Delta_A^*$  and  $\Delta_A$ :
  - (a) The toric variety  $B$  is encoded by the fan spanned by the  $A$ -Newton polytope,  $\Sigma_B \triangleleft \Delta_B^* := \Delta_A$ , so the  $B$ -Newton polytope is  $\Delta_B = \Delta_A^* = (\Delta_A)^\circ = (\Delta_B^*)^\circ$ .
  - (b) Anticanonical sections are encoded again encoded  $\Gamma(\mathcal{K}_B^*) = \bigoplus_{v_i} b_i \prod_j y_j^{\langle \mu_j | v_i \rangle + 1}$ , where  $v_i \in \mathbb{Z}^n \cap \Delta_B$  are lattice points and the Cox variables are  $y_j \mapsto \mu_j \in \Sigma_B^{(1)} \xrightarrow{1-1} \Delta_B^{*(1)}$ , one for each vertex of  $\Delta_B^*$ .

These definitions expose the *direct* relation to the “transposition mirror construction” [44, 55]:

$$f(x) \in \bigoplus_{\mu_j \in \Delta_A^{(1)}} a_j \left( \underbrace{\prod_{\nu_i \in \Delta_A^{*(1)}} x_i^{\langle \nu_i | \mu_j \rangle + 1}}_{\text{step 2}} \right) \xleftrightarrow{\circ} \bigoplus_{v_i \in \Delta_A^{*(1)}} b_i \left( \underbrace{\prod_{\mu_j \in \Delta_A^{(1)}} y_j^{\langle \mu_j | v_i \rangle + 1}}_{\text{step 4b}} \right) \ni g(y), \quad (4.1)$$

using that  $\Delta_B^* = \Delta_A$  and  $\Delta_B = \Delta_A^*$ , and having restricted to the vertices in both cases. In fact, in each of the two polytopes, any subset of lattice points the convex hull of which encloses the origin may be used [57, Appendix A], producing a web of multiple mirrors.

It is thus natural to ask: Starting from a non-weak-Fano toric variety,  $A$ , specified by a fan spanned by a non-convex polytope,  $\Sigma_A \triangleleft \Delta_A^*$ , what sort of space  $B$  is prescribed by a “minimal” adaptation of the above construction, so that the relations:

$$\begin{aligned} B: \Sigma_B \triangleleft \Delta_B^* = \Delta_A \quad \text{and} \quad \Delta_B = \Delta_A^* \triangleright \Sigma_A, \\ \text{so} \quad B \supset \{g(Y)=0\} = \tilde{\mathcal{X}} \xrightarrow{\text{mirror}} \mathcal{X} = \{f(X)=0\} \subset A, \end{aligned} \quad (4.2)$$

continue to hold even when  $\Delta_A^*$  is non-convex, so its transpolar  $\Delta_A$  is a self-crossing multotope rather than an ordinary polytope.

#### 4.2 The Transposed GLSM

**GLSM:** At face value, the prescription (4.1) provides the mirror-GLSM, requiring “merely” to read out the geometry. Given a left-hand side polynomial, we identify a transverse “minimal” part,  $f_0(X) = \sum_{j=1}^{n+1} \left( \prod_{i=1}^{n+r} X_i^{e_{ij}} \right)$ , with as many monomials as there are variables, and so the matrix of exponents,  $e_{ij} := \langle \mu_j | \nu_i \rangle + 1$ , is of maximal rank;  $f(X) - f_0(X)$  is treated as a deformation. The following procedure then constructs the mirror-GLSM:

1. Extending the “transposition construction” [44], the mirror-defining polynomial is simply the “transpose,”  $g_0(Y) = \sum_{i=1}^{n+r} \left( \prod_{j=1}^{n+1} Y_j^{e_{ji}} \right)$ , using  $\llbracket e_{ji} \rrbracket = \llbracket e_{ij} \rrbracket^T$ .

2. This  $g_0(Y)$  determines the  $U(1; \mathbb{C})^{\check{r}}$ -charges of the  $Y_j$  by the double requirement

$$\sum_{j=1}^{n+\check{r}} \check{q}_{aj} e_{ji} = -\check{q}_{a0} \stackrel{*}{=} \sum_{j=1}^{n+\check{r}} \check{q}_{aj}, \quad \check{q}_{aj} := \check{q}_a(Y_j) \quad \text{and} \quad \check{q}_{a0} := \check{q}_a(Y_0). \quad (4.3)$$

Aiming for a mirror-superpotential of the general form  $\widetilde{W} = Y_0 g(Y)$  where 2nd, the \*-labeled equality stipulates the gauge-invariance, anomaly cancellation and Ricci-flatness condition mirroring (1.4) on the transposed side.

3. Just like (1.4), the gauge-invariance, anomaly-cancellation and Ricci-flatness conditions (4.3) in the mirror model have a continuum of solutions. However, it is straightforward to find bases convenient for determining the  $U(1; \mathbb{C})^{\check{r}}$  gauge-symmetry breaking patterns, mirroring (2.4) and (3.9), and thus also the phase diagram of the mirror model, akin to the one in Figure 1.
4. Given the charges where  $g(Y) \in (\Pi Y) \cup \bigcup_j [\delta_j \Pi Y]$  is chosen from a (3.12)-like collection of  $Y$ -monomials of charge  $-\check{q}_{a0}$ . These 1st-order deformations of  $\Pi Y$ ,  $[\delta_j \Pi X] = [m_j(Y)(\partial_j \Pi Y)]$ , are again organized by their poset structure, mirroring that one in Figure 3.
5. From a chosen  $\check{q}_{aj}$ -basis, the mirror-analogue of (2.3),

$$\sum_{i=1}^{n+2} \check{q}_a(Y_j) \mu_j = -\check{q}_a(Y_0), \quad (4.4)$$

reverse-engineers the “vertices” in the poset constructed in the previous step, 4.

It is reassuring to find<sup>25</sup> that this procedure invariably reconstructs the generalized transposition-mirror relation (4.2) and the results of the combinatorially defined and computed *transpolar* relationship with the  $X$ -model, such as the  $\nabla$ -indicated correspondences in Figure 4—and for all non-convex and/or self-crossing VEX multitopes, just as it (of course) does for (convex) reflexive polytopes!

Consider, for proof-of-concept, the infinite sequence of  $F_m^{(3)}[c_1]$  GLSMs, where retaining only the “vertex”-monomials in Figure 3 simplifies the superpotential to

$$X_0 \left( X_1^3 (X_4^{2+2m} + X_5^{2+2m}) + X_2^3 (X_4^{2-m} + X_5^{2-m}) + X_3^3 (X_4^{2-m} + X_5^{2-m}) \right), \quad (4.5)$$

with the matrix of exponents (reading row-wise by monomials),

$$\llbracket e_{ij} \rrbracket = \begin{bmatrix} 3 & 0 & 0 & 2+2m & 0 \\ 3 & 0 & 0 & 0 & 2+2m \\ 0 & 3 & 0 & 2-m & 0 \\ 0 & 3 & 0 & 0 & 2-m \\ 0 & 0 & 3 & 2-m & 0 \\ 0 & 0 & 3 & 0 & 2-m \end{bmatrix}. \quad (4.6)$$

In step 2, the twin conditions (4.3) for the transpose matrix of exponents of (4.5) then defines:

	$Y_0$	$Y_1$	$Y_2$	$Y_3$	$Y_4$	$Y_5$	$Y_6$
$\check{q}_1$	$9(m-2)$	0	$3(m-2)$	$-2m-5$	$5m-1$	$2(m-2)$	$m-2$
$\check{q}_2$	$9(m-2)$	$3(m-2)$	0	$4m+1$	$-m-7$	$2(m-2)$	$m-2$
$\check{q}_3$	$12(m+1)$	$m+4$	$3m$	0	$4(m+1)$	$2(m+1)$	$2(m+1)$
$\check{q}_4$	$6(m+2)$	$2m$	4	$2(m+2)$	0	$2(m+1)$	2
$\check{q}_5$	6	$3-m$	$m-1$	$-2m$	$2(m+1)$	0	2
$\check{q}_6$	$6(m+1)$	$m+1$	$m+1$	0	$2(m+1)$	$2(m+1)$	0

(4.7)

<sup>25</sup>This is an “experimental fact,” obtained for many dozens of  $n = 2, 3$  examples (including some infinite sequences, such as starting with (3.1) for arbitrary  $m$ ) — but I am not aware of a formal, rigorous proof.

As specified in step 3, these  $\check{q}_a$ -candidates are chosen so  $\check{q}_i(Y_i)=0$ —analogous to the choices (2.4)—which then describes the phase-space of the model, following §§ 2.1–2.2. The rank of the  $6 \times 7$  matrix of charges (4.7) is 3, informing us that the transposed GLSM model has a  $U(1; \mathbb{C})^3$  gauge symmetry, generated by any three of these  $\check{q}_a$ -charges, which provides for non-trivial differences as compared with the  $(n, m) = (2, 3)$  special case shown in Ref. [56, § 3.3]. With these, the remaining two steps, 4–5 are straightforward.

This generalizes considerably beyond the by now well-studied transposition-mirror construction for “invertible” defining polynomials [44, 45, 49, 116–126]: the  $5 \times 6$  matrix of exponents (4.6) is neither square nor of maximal rank. Incidentally,  $\text{rank}[[e_{ij}]] = 4$  implies that restricting (4.5) to four monomials (which in the Figure 4 plot span an origin-enclosing simplex) in four variables (by setting  $X_1 \rightarrow 1$ ) does result in an “invertible” (albeit Laurent) special case. In fact, replacing (4.5) with any other selection of four monomials from the poset in Figure 3 that span an origin-enclosing 3-simplex in the  $\Delta_{F_5^{(3)}}$ -point set also results in an “invertible” Laurent special case; for worked-out examples, see Ref. [56, 57]. This plethora of choices grows combinatorially with  $(n, m)$  and indicates that a full  $F_m^{(n)}[c_1]$ -GLSM may also be thought of as a *generating function* for such “invertible” Laurent models.

The foregoing discussion then justifies the expectation that the so-constructed mirror-GLSM can describe both the mirror Calabi–Yau model,  $\check{\mathcal{X}}$ , and owing to the observation in Remark 1.2 also (a choice of) the ambient space,  $B$ , in which that mirror is the hypersurface,

$$B \supset \check{\mathcal{X}} =: \{g(Y) = 0\} \xleftarrow{\text{transpose}} \{f(X) = 0\} := \mathcal{X} \subset A, \quad (4.8)$$

justifying the interest in candidate ambient spaces,  $B$ , corresponding to the self-crossing multitopes, such as  $\Delta_{F_5^{(3)}}$ ,  $\Delta_{F_{4,1}^{(3)}}$  and  $\Delta_{F_{3,2}^{(3)}}$  in Figure 4, and the multifans they span.

### 4.3 Ambient Unitary Torus Manifolds

Since the explicitly continuous deformation families of generalized complete intersections of Calabi–Yau manifolds in products of projective spaces [54, 95, 96] manifestly include the Hirzebruch  $n$ -fold scrolls (3.1) and  $F_m^{(n)}$  with arbitrarily high (“taxicab”) magnitude  $|\vec{m}|$  as factors in the ambient space, “the cat is out of the bag”: Discrete deformations of the  $F_m^{(n)} \approx_{\mathbb{R}} F_{m-n}^{(n)}$  kind may well be wide-spread,<sup>26</sup> requiring the inclusion of ambient spaces (and their suitable hypersurfaces) corresponding to flip-folded or otherwise self-crossing multitopes such as  $F_5^{(3)}$ ,  $F_{4,1}^{(3)}$  and  $F_{3,2}^{(3)}$  in Figure 4.

Such self-crossing multitopes have been studied for considerable time—in *symplectic geometry* [113–115]—which is in fact encouraging, given that mirror duality maps complex structure to (special) symplectic structure [51–53]. They span the flip-folded *multifans* that also have a long history [64–75]. Such fans are known to encode “half-dimensional”  $(S^1)^n$ -action (transformation) on the underlying real  $2n$ -dimensional *torus manifold*,  $\mathcal{M}$ , which then contains multifan-encoded “characteristic submanifolds,”  $M_i$ , fixed under some subgroup of the “compact torus” group,  $T := (S^1)^n$ . These  $M_i$  are analogous to the Cox divisors (in real codimension-2) and other submanifolds indicated by the various cones in the fan encoding the variety.

For purposes of building a GLSM (§§ 1.2 and 4.2) with such a torus manifold as the ambient space, a subclass is needed that (to start with) accommodates:

1. complex-valued local coordinates (the  $X_i$  and  $Y_j$  chiral superfields are  $\mathbb{C}$ -valued), and

<sup>26</sup>Whereas among the complex 2-dimensional candidates for a factor in a “well-known” ambient space only the Hirzebruch surfaces exhibit the discretely variable complex structure [18, 102], higher-dimensional varieties should be more amenable to such features.

- an anticanonical  $\mathbb{C}$ -line bundle with  $\mathbb{C}$ -valued sections the zero-locus of which to define Calabi–Yau hypersurfaces of our ultimate interest.

Both of these can be satisfied by so-called *unitary torus manifolds* (UTMs), [64–66].

By definition, the *unitary* (i.e., *weakly almost complex*) structure on a *real*  $2n$ -dimensional manifold,  $\mathcal{M}$ , is a complex structure on its ( $\mathbb{R}^{2r}$ -extended) *stable tangent bundle*,  $\mathcal{T}_{\mathcal{M}} \oplus \mathbb{R}^{2r}$  for some  $0 \leq r \in \mathbb{Z}$ ; almost complex manifolds are the  $r = 0$  special case. Here,  $\mathbb{R}^{2r}$  denotes the trivial bundle over  $\mathcal{M}$ , which is on a UTM also invariant under its “half-dimensional”  $(S^1)^n$ -transformations. In particular, the (real) tangent bundle,  $\mathcal{T}_{\mathcal{M}}$ , turns out to be a quotient of the direct sum,  $\bigoplus_{i=1}^{n+r} L_i$ , of  $\mathbb{C}$ -line bundles associated with the vertex-ray generators of the multifan,  $\Sigma_{\mathcal{M}}$ ,—just like in complex-algebraic toric varieties, where this quotient refers to the so-called Euler sequence [18, 30]. However—and unlike in a complex-algebraic toric varieties, (1) these  $L_i$  are  $\mathbb{C}$ -valued *smooth* (not a priori holomorphic) line bundles, and (2) the quotienting map,  $\bigoplus_{i=1}^{n+r} L_i \rightarrow \mathcal{T}_{\mathcal{M}}$ , is in general not guaranteed to be  $(\mathbb{C}^* \supset S^1)^n$ -equivariant compatibly with the complex structure of the line bundles. That is, the quotienting map,  $\bigoplus_{i=1}^{n+r} L_i \rightarrow \mathcal{T}_{\mathcal{M}}$  may not have a  $T$ -equivariant inverse, so as to identify  $\bigoplus_{i=1}^{n+r} L_i$  with  $\mathcal{T}_{\mathcal{M}} \oplus \mathbb{R}^{2r}$  equivariantly.<sup>27</sup>

Nevertheless, the top exterior power of this direct sum *does* define a  $\mathbb{C}$ -valued “anticanonical bundle,”  $\mathcal{K}_{\mathcal{M}}^* := \wedge (\mathcal{T}_{\mathcal{M}} \oplus \mathbb{R}^{2r})$ , and UTMs moreover have the  $T$ -equivariant Chern class,  $c^T(\mathcal{M}) := \prod_i (1 + \xi_i)$ , generated by  $\xi_i = c_1^T(L_i) \in H_T^2(\mathcal{M})$ , so  $c_1^T(\mathcal{K}_{\mathcal{M}}^*) = \sum_i \xi_i$  [64, 66]. Furthermore, unless the  $T$ -equivariant Todd class vanishes,  $\mathcal{M}$  is *cohomologically symplectic*: there exists an element  $\Xi \in H^2(\mathcal{M})$  such that  $\Xi^n \neq 0$  [64, Cor. 4.3]; this  $\Xi$  is the unitary equivalent of a Kähler class, with  $\Xi^n$  the Kähler volume-form. The *orientation* (winding or wrapping index),  $w(\sigma) = +1$  ( $-1$ ), of an  $n$ -cone,  $\sigma \in \Sigma_{\mathcal{M}}$ , indicates (dis)agreement in the affine chart  $\mathcal{U}_{\sigma} \subset \mathcal{M}$  between the orientation induced from the complex structure of  $\mathcal{T}_{\mathcal{M}} \oplus \mathbb{R}^{2r}$  and that of  $\mathcal{M}$  itself. The  $w(\sigma)$ -signed degree of both a cone and its facet,  $\sigma = \sphericalangle(\theta)$ ,<sup>28</sup> determines a so-called Duistermaat–Heckman measure over the multifan  $\Sigma_{\mathcal{M}}$  [65, 66] (see also [128]), and an *omniorientation* on  $\mathcal{M}$  [67, 73, 74, 129]. The  $w(\sigma)$ -sign of cone and facet degrees turns out to be the *only* extension of standard complex-algebraic toric geometry computations that is necessary and sufficient in the various computations of Refs. [55–59].

**Relations to GLSMs:** Section 1.2 started with GLSMs containing  $n+r$  complex (chiral,  $(2, 2)$ -super)fields,  $X_i$ , each with its own, a priori independent phase-transformation,  $X_i \rightarrow \lambda_i X_i$ , generating the  $\{\lambda_i \neq 0, i = 1, \dots, (n+r)\} = (\mathbb{C}^*)^{n+r}$  complex-torus actions. The  $U(1; \mathbb{C})^r \approx (\mathbb{C}^*)^r$ -subgroup was gauged, specifying the partitioning of the  $X$ -field space into separate gauge-orbits (see § 2.1), leaving the remaining  $(\mathbb{C}^*)^n$ -transformation to characterize the fan of the toric  $n$ -fold. For example, in (2.4), the top three rows correspond to this latter, un-gauged  $(\mathbb{C}^*)^3$ -transformation on the toric 3-fold,  $F_m^{(3)}$ , while any two of the  $q_a$ -rows specify the gauged  $U(1; \mathbb{C})^2 \approx (\mathbb{C}^*)^2$ -transformation.

The  $(S^1)^n$ -“circle transformation” specified by the multifan,  $\Sigma_{\mathcal{M}}$ , in UTMs may be identified with the phase-angle transformation implemented by multiplying with  $\lambda \in \mathbb{C}^*$  while restricting to  $|\lambda| = 1$ , and leaving any accompanying “radial scaling” by multiplying with  $|\lambda| \in \mathbb{R}_+$  simply unspecified.<sup>29</sup> Conversely,

<sup>27</sup>I thank Amin Gholampour for explaining to me the  $T$ -equivariance subtlety.

<sup>28</sup>The degree of a  $k$ -face,  $d(\theta^{(k)}) := (k+1)! \cdot \text{Vol}_{k+1}(\theta^{(k)})$ , is the  $(k+1)$ -fold volume of the *star-pyramid* over  $\theta^{(k)}$  [48]. Faces with  $|d(\theta)| > 1$  and the cones they span encode  $(\mathbb{C}^n / \mathbb{Z}_{d(\theta)})$ -charts in the toric space; their desingularization is encoded by a subdivision of the cone. For simplicity, we tacitly identify the torus manifold-specific orientation-function with the multifan-specific  $w$ -function [64–66]. Subtleties in “reading” a multifan (affecting its fit for our application) are exemplified by the case of  $S^4$  [127].

<sup>29</sup>This polar-coordinate identification of “radial” and “circular” part of the  $\mathbb{C}^*$ -transformation is referred to as the “locally standard”  $\mathbb{C}^*$ -transformation, identifying in turn the chart,  $\mathcal{U}_{\sigma}$ , of every unit-degree cone  $\sigma \in \Sigma_{\mathcal{M}}$  with an affine copy of  $\mathbb{C}^n$ —up to chart-wise conjugation.

complex-algebraic toric varieties may be regarded as UTMs in which a *unique*  $\mathbb{R}_+$ -“radial scaling” is associated with for each  $S^1$ -“circle transformation,” determined by the overall complex structure of the variety, and combining them, into the hallmark complex toric transformation,  $S^1 \times \mathbb{R}_+ \rightarrow \mathbb{C}^*$ . This comparison provides for the fact that there exists a *continuum* of UTMs corresponding to any given multifan. More generally and starting from a multifan  $\Sigma$ -specified  $(S^1)^n$ -transformations, we seek a real  $2n$ -dimensional UTM,  $\mathcal{M}$ , corresponding to  $\Sigma$ , which admits *some suitable*  $S^1 \leftrightarrow \mathbb{R}_+$  association for each of the  $n+r$  generators to correspondingly extend each  $S^1 \rightsquigarrow \mathbb{C}^*$ -transformation that will:

1. coincide with the canonical association and  $\mathbb{C}^*$ -transformation within the algebraically “rigid” subclass of complex-algebraic toric varieties,<sup>30</sup>
2. extend to (some of the continuum of) UTMs corresponding to the VEX multifans produced by the transposition mirror construction in §§ 4.1–4.2 [55–59],
3. be consistent with all physics-relevant (mostly cohomology ring, but also *metric* [33–38]) computation hallmarks of mirror symmetry,

and ultimately,

4. be consistent also with geometric (conifold and other) transitions.

While this may seem like a “tall order” and too restrictive to meaningfully extend the framework of complex-algebraic toric geometry (and so leave models such as  $F_{\vec{m}}^{(n)}[c_1]$  with  $|\vec{m}| \geq 3$  with no mirror reflexion), the fact that there exists a *continuum* of UTMs corresponding to every multifan gives hope. This does however make the task of identifying the “right” (possibly non-complex-algebraic) UTMs to serve as the ambient space “ $B$ ” in Eqs. (4.2) and (4.8) akin to seeking a needle in a sea.

**A Likely Subclass:** To this end, let us close by calling attention to a very special subclass of UTMs, so-called *topological torus manifolds* (TTMs) [71], which seem excellent candidates as they exhibit several promising features:

1. Each TTM is uniquely specified by a *topological fan*, defined over the “ground field”  $\mathcal{R} \approx \mathbb{C} \times \mathbb{Z}$ , conveniently parametrized as  $\begin{bmatrix} b & 0 \\ c & v \end{bmatrix} \in \mathcal{R}$ , with  $b, c \in \mathbb{R}$  and  $v \in \mathbb{Z}$ :
  - (a) Each complex-torus  $0 \neq \lambda \in \mathbb{C}^*$ -transformation is  $\mathcal{R}$ -parametrized:

$$\lambda \cdot X := |\lambda|^b e^{i(c \log |\lambda| + v \arg(\lambda))} X, \quad (4.9)$$

where  $\arg(\lambda) := \frac{1}{2i} \log(\lambda/\lambda^*)$  is the phase-angle of  $\lambda$ ;

such that:

- (b) the  $b$ -projection,  $\Sigma_{\mathcal{M}}^b$ , is a plain, non-self-crossing fan in  $\mathbb{R}^n$ , generated by a continuous choice of (not necessarily lattice)  $\mathbb{R}^n$ -vectors;
  - (c) the  $v$ -projection,  $\Sigma_{\mathcal{M}}^v$ , is a  $\mathbb{Z}^n$ -lattice multifan in  $\mathbb{R}^n$ .
2. Restricting to  $c=0$  and  $b=v \in \mathbb{Z}$  recovers the familiar complex-algebraic toric varieties as a special case of TTMs. Omitting the  $(b, c)$ -information “loosens” TTMs into UTMs.
  3. The cohomology rings of the TTM  $\mathcal{M}$  are completely determined solely by its  $v$ -projection multifan,  $\Sigma_{\mathcal{M}}^v$ .

This last feature is especially encouraging, since it insures that there exists a  $(b, c)$ -continuum of TTMs the cohomology ring of which reproduces all the various computations in Refs. [55–59].

<sup>30</sup>Danilov’s characterization as “frigid toric crystals” comes to mind [26, p. 100].

It remains to determine which (if any) of these  $\mathcal{R}$ -extensions of each VEX multifan  $\Sigma_{\mathcal{M}}^v$  can guarantee the underlying TTM to admit the requisite  $\mathbb{C}$ -valued bundles, with adequate  $\mathbb{C}$ -valued sections, so as to define as their zero locus the Calabi–Yau hypersurfaces of our ultimate interest (see Refs. [57, 58] for a catalogue of claims and conjectures with complementary justification)—and this is currently actively explored; see, e.g., [130, 131].

## 5 Conclusions and Outlook

In this sequel to Ref. [59], the overall general structure of worldsheet sigma models is reconsidered with the specific focus on constructing pairs of worldsheet models the ground states of which are transposition-mirror Calabi–Yau hypersurfaces (4.8)—even when one of them is a hypersurface in a non-weak-Fano variety,  $\mathcal{X} := \{f(X)=0\} \subset A$ . Its transposition-mirror is then constructed as a hypersurface,  $\tilde{\mathcal{X}} := \{g(Y)=0\} \subset B$ , in an ambient space,  $B$ , that cannot be a complex-algebraic toric variety, but would seem to be a special type of a unitary torus manifold (UTM), the precise type of which remains to be determined, so-called topological torus manifolds (TTMs) providing promising candidates.

To help with this determination, § 4.2 details the construction of the transposed-GLSM, thus providing the “bill of materials” required in this construction, and which a usable candidate UTM,  $\mathcal{M}$ , must be able to provide. In particular, UTMs do admit  $\mathbb{C}$ -valued line bundles with  $\mathbb{C}$ -valued sections that may serve as local coordinates on the ambient space, and their top exterior power defines the anticanonical  $\mathbb{C}$ -line bundle with  $\mathbb{C}$ -valued sections the zero-locus of which to define Calabi–Yau hypersurfaces of our ultimate interest.

However, these  $\mathbb{C}$ -valued line bundles on a UTM, or even on the additionally qualified TTM, are a priori defined as *smooth* rather than holomorphic bundles, and it has been conjectured that flip-folded regions (composed of  $w(\sigma) = -1$  cones) in the multifan encode obstructions to a global (almost) complex structure [57]: A top-dimensional unit-degree cone,  $\sigma$ , in an  $n$ -dimensional (multi)fan,  $\Sigma_{\mathcal{M}}$  corresponds to a  $\mathbb{C}^n$ -like local chart,  $\mathcal{U}_{\sigma} \subset \mathcal{M}$ , and the sign of  $w(\sigma)$  determines whether its orientation agrees with the unitary structure (the complex structure of  $\mathcal{T}_{\mathcal{M}} \oplus \mathbb{R}^{2r}$ ) or is opposite.

This prompts the conjecture [57] that when two adjacent cones,  $\sigma_i, \sigma_j$ , flip-fold ( $w(\sigma_i)w(\sigma_j) < 0$ ) across their common facet  $\varsigma_{ij} = \sigma_i \cap \sigma_j$ , a chart-wise local complex structure *need not* transfer holomorphically from  $\mathcal{U}_{\sigma_i}$  to  $\mathcal{U}_{\sigma_j}$ : With respect to the global *unitary structure* of  $\mathcal{M}$  (= complex structure of  $\mathcal{T}_{\mathcal{M}} \oplus \mathbb{R}^{2r}$ ), if  $\mathcal{U}_{\sigma} \approx_{\mathbb{C}} \mathbb{C}^n$  for  $w(\sigma) > 0$  then  $\mathcal{U}_{\sigma'} \approx_{\mathbb{C}} \overline{\mathbb{C}^n}$  for  $w(\sigma') < 0$ —if both charts admit a “locally standard”  $\mathbb{C}^*$ -transformation. Then, flip-folded parts of a multifan encode chart-wise conjugation local obstructions to a complex structure on their glued union,  $\mathcal{U}_{\sigma_i} \cup_{\varsigma_{ij}} \mathcal{U}_{\sigma_j}$ . However, as seen in Figure 4: both side-panes of  $\Delta_{F_5^{(3)}}$ , the back-pane of  $\Delta_{F_{4,1}^{(3)}}$ , and the front- and back-panes of  $\Delta_{F_{3,2}^{(3)}}$  are themselves self-crossing, and so presumably cannot correspond to “locally standard”  $\mathbb{C}^*$ -transformation in the corresponding  $\mathcal{U}_{\sigma} \approx_{\mathbb{R}} \mathbb{R}^4$ -charts, so a more detailed (rigorous) analysis is needed to establish *if* and *precisely how* do UTMs with flip-folded multifans fail to be (almost) complex.

**Remark 5.1:** In lieu of such more precise analysis, and showcased by the multitopes  $\Delta_{F_5^{(3)}}$ ,  $\Delta_{F_{4,1}^{(3)}}$  and  $\Delta_{F_{3,2}^{(3)}}$  that rather prominently feature flip-folded “extensions” (depicted as the frontmost, “hanging” panes in Figure 4), we may only infer that a (chart-wise glued) almost complex structure *may* have local obstructions in a UTM, in the local charts corresponding to the flip-folded regions in its multifan,  $\Sigma_{\mathcal{M}}$ . ▀

If a UTM,  $\mathcal{M}$ , does have such obstructions to an almost complex structure and the anticanonical hypersurface of our ultimate interest,  $\mathcal{X} \in \mathcal{M}[c_1]$ , intersects it,  $\mathcal{X}$  itself “inherits” the obstruction, and so cannot be almost complex—which would imply that the definitions (1.1) and (1.2) must be modified. How

this happens and whether (and how) string theory may accommodate such “defects”—or if they turn out to break the target space supersymmetry guaranteed by this complex structure—is a tantalizing question, which however remains open for now. In turn, such “defects” may also turn out to be innocuous if an ambient UTM (from a *continuum* that corresponds to any given multifan) can be found where  $\mathcal{X} \subset \mathcal{M}$  “misses” the obstruction locus.

That such “defects” are localized is most easily seen by considering the 2-dimensional case of the (extended, complete) Newton multigon of  $F_3^{(2)}$  [56, 58], depicted at left:

$$\begin{bmatrix}
 -1 & 1 & 0 & 0 & 0 & 0 & 0 & 0 & 1 \\
 1 & -2 & 1 & 0 & 0 & 0 & 0 & 0 & 0 \\
 0 & 1 & 0 & 1 & 0 & 0 & 0 & 0 & 0 \\
 0 & 0 & 1 & -3 & 1 & 0 & 0 & 0 & 0 \\
 0 & 0 & 0 & 1 & -1 & 1 & 0 & 0 & 0 \\
 0 & 0 & 0 & 0 & 1 & -2 & 1 & 0 & 0 \\
 0 & 0 & 0 & 0 & 0 & 1 & -2 & 1 & 0 \\
 0 & 0 & 0 & 0 & 0 & 0 & 1 & -2 & 1 \\
 1 & 0 & 0 & 0 & 0 & 0 & 0 & 1 & -2
 \end{bmatrix}
 \tag{5.1}$$

$C_1^2(Z) = 3$  and  $C_2(Z) = 9$

As specified in (4.2) and (4.8), the Newton multigon of  $F_3^{(2)}$  is equated with the multifan-spanning multigon of the UTM,  $B = \nabla F_3^{(2)}$ , in which the transpose-mirror Calabi–Yau hypersurface (here, a 2-torus) is to be identified. Depicted on the right-hand side is the polygon spanning the fan of a complex-algebraic (albeit non-weak-Fano) toric variety,  $Z$ , together with the intersection matrix of its (lattice point corresponding) divisors, starting with  $D_{\nu_1}$  and encircling the origin in (arrow-indicated) CCW order. The  $\Sigma_{\nabla F_3^{(2)}}$  multifan differs from the  $\Sigma_Z$  fan only in the additional  $\nu_3$ -ray that subdivides the  $\nu_{2^*}$ -cone, but not within it, as would be required in standard complex-algebraic toric geometry. Consequently,  $\nabla F_3^{(2)}$  is not a standard blowup of the toric variety  $Z$ ; nevertheless, the difference between the two manifolds is localizable to the  $\nu_3$ -encoded exceptional  $\mathbb{P}^1$ -like set—which then (with its normal space) obstructs a complex structure on  $\nabla F_3^{(2)}$ . This makes  $\nabla F_3^{(2)}$  (and all UTMs corresponding to flip-folded self-crossing multitopes) a priori *pre-complex*—so named mirroring *pre-symplectic manifolds*, wherein the symplectic structure may degenerate at real codimension-2 locations [57–59].

In turn, the UTM corresponding to the multifan spanned by the multitope  $\Delta_{F_3^{(2)}}$  in (5.1) may also be regarded as a blowdown of a UTM,  $\mathcal{Z}$ , which is *almost complex* by [64, Thm. 5.1] as it corresponds to the double-winding multifan spanned by the star-shaped multitope:

$$\begin{bmatrix}
 -1 & 1 & 0 & 0 & 0 & 0 & 0 & 0 & 0 & 0 & 0 & 0 & 1 \\
 1 & -2 & 1 & 0 & 0 & 0 & 0 & 0 & 0 & 0 & 0 & 0 & 0 \\
 0 & 1 & 2 & 1 & 0 & 0 & 0 & 0 & 0 & 0 & 0 & 0 & 0 \\
 0 & 0 & 1 & 1 & 1 & 0 & 0 & 0 & 0 & 0 & 0 & 0 & 0 \\
 0 & 0 & 0 & 1 & 2 & 1 & 0 & 0 & 0 & 0 & 0 & 0 & 0 \\
 0 & 0 & 0 & 0 & 1 & -2 & 1 & 0 & 0 & 0 & 0 & 0 & 0 \\
 0 & 0 & 0 & 0 & 0 & 1 & -1 & 1 & 0 & 0 & 0 & 0 & 0 \\
 0 & 0 & 0 & 0 & 0 & 0 & 1 & -2 & 1 & 0 & 0 & 0 & 0 \\
 0 & 0 & 0 & 0 & 0 & 0 & 0 & 1 & -2 & 1 & 0 & 0 & 0 \\
 0 & 0 & 0 & 0 & 0 & 0 & 0 & 0 & 1 & -2 & 1 & 0 & 0 \\
 0 & 0 & 0 & 0 & 0 & 0 & 0 & 0 & 0 & 1 & -2 & 1 & 0 \\
 1 & 0 & 0 & 0 & 0 & 0 & 0 & 0 & 0 & 0 & 1 & -2 & -1
 \end{bmatrix}
 \tag{5.2}$$

$C_1^2(\mathcal{Z}) = 13$  and  $C_2(\mathcal{Z}) = 11$ , so  $\text{Td}(\mathcal{Z}) = 2$

With the Todd genus = 2, this almost complex UTM,  $\mathcal{X}$ , cannot possibly be a complex-algebraic toric variety, which resonates with of Danilov’s prescient remark; see footnote 30. The sequence of blowdown-like local surgeries (5.1)–(5.2),  $\mathcal{X} \dashrightarrow \mathbb{V}F_3^{(2)} \dashrightarrow Z$ , should aid in determining the geometry of  $\mathbb{V}F_3^{(2)}$  in terms of the almost complex UTM,  $\mathcal{X}$ , and the non-weak-Fano toric variety,  $Z$ . In fact, this local surgery sequence provides a template and a general prescription to describe the geometry of all UTMs corresponding to flip-folded multitudes and multifans. However, I defer this analysis to a subsequent endeavor.

— o —

In conclusion, this note examines the worldsheet (2, 2)-supersymmetric GLSM constructions featuring explicitly continuous deformation families of Hirzebruch scrolls with (secondary) deformation families of Calabi–Yau hypersurfaces in each scroll. When those ambient scrolls are not even weak-Fano, the transposition-mirrors of the Calabi–Yau hypersurfaces are by a transposed GLSM construction nevertheless indicated as hypersurfaces in non-algebraic ambient spaces identified as (suitably  $\mathbb{C}$ -ringed) unitary torus manifolds, the precise geometry and physics consequences of which remain to be determined.

**Acknowledgments:** I am deeply thankful to Per Berglund for decades of collaborations including on many of the topics discussed here, to Mikiya Masuda for guidance through unitary and topological torus manifolds, and to Yong Cui, Amin Gholampour, Zengui Han for convincing me of the TTMs’ promising nature, and to Elijah Sheridan for insightful discussions about vexing. I am grateful to the Mathematics Department of the University of Maryland, and the Physics Department of the University of Novi Sad, Serbia, for recurring hospitality and resources.

## References

- [1] M. B. Green and J. H. Schwarz, “Anomaly cancellation in supersymmetric D=10 gauge theory and superstring theory,” *Phys. Lett.* **B149** (1984) 117–122.
- [2] D. J. Gross, J. A. Harvey, E. J. Martinec, and R. Rohm, “The heterotic string,” *Phys. Rev. Lett.* **54** (1985) 502–505.
- [3] P. Candelas, G. T. Horowitz, A. Strominger, and E. Witten, “Vacuum configurations for superstrings,” *Nucl. Phys.* **B258** (1985) 46–74.
- [4] D. H. Friedan, “Nonlinear models in  $2+\epsilon$  dimensions,” *Phys. Rev. Lett.* **45** (1980) 1057.
- [5] D. H. Friedan, “Nonlinear models in  $2+\epsilon$  dimensions,” *Ann. Phys.* **163** (1985) 318–419.
- [6] J. Polchinski, *String theory. Vol. 1: An introduction to the bosonic string*. Cambridge Monographs on Mathematical Physics. Cambridge University Press, Dec., 2007.
- [7] J. Polchinski, *String theory. Vol. 2: Superstring theory and beyond*. Cambridge Monographs on Mathematical Physics. Cambridge University Press, Dec., 2007.
- [8] I. B. Frenkel, H. Garland, and G. J. Zuckerman, “Semiinfinite cohomology and string theory,” *Proc. Nat. Acad. Sci.* **83** (1986) 8442.
- [9] M. J. Bowick and S. G. Rajeev, “String theory as the Kähler geometry of loop space,” *Phys. Rev. Lett.* **58** (1987) 535.
- [10] M. J. Bowick and S. G. Rajeev, “The holomorphic geometry of closed bosonic string theory and  $\text{Diff } S^1/S^1$ ,” *Nucl. Phys.* **B293** (1987) 348.
- [11] M. J. Bowick and S. Rajeev, “The complex geometry of string theory and loop space,” in *Johns Hopkins Workshop on Current Problems in Particle Theory*, Y.-S. Duan, G. Domókos, and S. Kövesi-Domókos, eds. World Sci. Publishing, Singapore, July, 1987.
- [12] P. Oh and P. Ramond, “Curvature of Superdiff  $S^1/S^1$ ,” *Phys. Lett.* **B195** (1987) 130–134.
- [13] D. Harari, D. K. Hong, P. Ramond, and V. G. J. Rodgers, “The superstring  $\text{Diff } S^1/S^1$  and holomorphic geometry,” *Nucl. Phys.* **B294** (1987) 556–572.
- [14] K. Pilch and N. P. Warner, “Holomorphic structure of superstring vacua,” *Class. Quant. Grav.* **4** (1987) 1183.
- [15] M. J. Bowick and S. G. Rajeev, “Anomalies and curvature in complex geometry,” *Nucl. Phys.* **B296** (1988) 1007–1033.

- [16] M. J. Bowick and A. Lahiri, “The Ricci curvature of  $\text{diff } S^1/\text{SL}(2, R)$ ,” *J. Math. Phys.* **29** (1988) 1979.
- [17] M. J. Bowick and K.-Q. Yang, “String equations of motion from vanishing curvature,” *Int. J. Mod. Phys. A* **6** (1991) 1319–1334.
- [18] T. Hübsch, *Calabi–Yau Manifolds: a Bestiary for Physicists*. World Scientific Pub. Europe Ltd., London, UK, 2nd ed., 2024. (subst. update of the 1st ed., 1992, World Scientific Pub.).
- [19] E. Witten, “Phases of  $N = 2$  theories in two-dimensions,” *Nucl. Phys.* **B403** (1993) 159–222, [hep-th/9301042](#).
- [20] D. R. Morrison and M. R. Plesser, “Summing the instantons: Quantum cohomology and mirror symmetry in toric varieties,” *Nucl. Phys.* **B440** (1995) 279–354, [arXiv:hep-th/9412236](#) [hep-th].
- [21] P. S. Aspinwall, T. Bridgeland, A. Craw, M. R. Douglas, A. Kapustin, G. W. Moore, M. Gross, G. Segal, B. Szendrői, and P. M. H. Wilson, *Dirichlet branes and mirror symmetry*, vol. 4 of *Clay Mathematics Monographs*. AMS, Providence, RI, 2009. <http://people.maths.ox.ac.uk/cmi/library/monographs/cmim04c.pdf>.
- [22] E. Sharpe, “A survey of recent developments in GLSMs,” *Int. J. Mod. Phys. A* **39** no. 33, (Jan., 2024) 2446001, [arXiv:2401.11637](#) [hep-th].
- [23] M. Kreuzer and H. Skarke, “Complete classification of reflexive polyhedra in four-dimensions,” *Adv. Theor. Math. Phys.* **4** (2000) 1209–1230, [arXiv:hep-th/0002240](#).
- [24] M. Kreuzer and H. Skarke, “Calabi–Yau data.” 2000. <http://hep.itp.tuwien.ac.at/~kreuzer/CY/>.
- [25] P. Griffiths and J. Harris, *Principles of algebraic geometry*. Wiley Classics Library. John Wiley & Sons Inc., New York, 1978.
- [26] V. I. Danilov, “The geometry of toric varieties,” *Russian Math. Surveys* **33** no. 2, (1978) 97–154. <http://stacks.iop.org/0036-0279/33/i=2/a=R03>.
- [27] T. Oda, *Convex Bodies and Algebraic Geometry: An Introduction to the Theory of Toric Varieties*. A Series of Modern Surveys in Mathematics. Springer, 1988.
- [28] W. Fulton, *Introduction to Toric Varieties*. Annals of Mathematics Studies. Princeton University Press, 1993.
- [29] G. Ewald, *Combinatorial Convexity and Algebraic Geometry*. Springer Verlag, 1996.
- [30] D. A. Cox, J. B. Little, and H. K. Schenck, *Toric Varieties*, vol. 124 of *Graduate Studies in Mathematics*. American Mathematical Society, 2011.
- [31] D. A. Cox and S. Katz, *Mirror Symmetry and Algebraic Geometry*, vol. 68 of *Mathematical Surveys and Monographs*. American Mathematical Society, Providence, RI, 1999.
- [32] A. Constantin, Y.-H. He, and A. Lukas, “Counting string theory standard models,” *Phys. Lett. B* **792** (2019) 258–262, [arXiv:1810.00444](#) [hep-th].
- [33] G. Butbaia, D. Mayorga Peña, J. Tan, P. Berglund, T. Hübsch, V. Jejjala, and C. Mishra, “Physical Yukawa couplings in heterotic string compactifications,” *Adv. Theor. Math. Phys.* **28** no. 8, (2024) 2783–2822, [arXiv:2401.15078](#) [hep-th].
- [34] A. Constantin, C. S. Fraser-Taliente, T. R. Harvey, A. Lukas, and B. Ovrut, “Computation of quark masses from string theory,” *Nucl. Phys. B* **1010** (2024) 116778, [arXiv:2402.01615](#) [hep-th].
- [35] P. Berglund, G. Butbaia, T. Hübsch, V. Jejjala, D. Mayorga Peña, C. Mishra, and J. Tan, “Precision String Phenomenology,” *Phys. Rev. D* **111** (July, 2025) 086007, [arXiv:2407.13836](#) [hep-th].
- [36] A. Constantin, C. S. Fraser-Taliente, T. R. Harvey, L. T. Y. Leung, and A. Lukas, “Quark masses and mixing in string-inspired models,” *JHEP* **06** (2025) 175, [arXiv:2410.17704](#) [hep-th].
- [37] G. Butbaia, D. Mayorga Peña, J. Tan, P. Berglund, T. Hübsch, V. Jejjala, and C. Mishra, “cymc: Calabi–Yau Metrics, Yukawas, and Curvature,” *JHEP* **03** (2025) 28, [arXiv:2410.19728](#) [hep-th].
- [38] A. Rahman, “GlobalCY I: A JAX framework for globally defined and symmetry-aware neural Kähler potentials,” [arXiv:2604.11404](#) [hep-th].
- [39] A. Sen, “(2, 0) Supersymmetry and Space-Time Supersymmetry in the Heterotic String Theory,” *Nucl. Phys. B* **278** (1986) 289–308.
- [40] S. B. Giddings, J. Polchinski, and A. Strominger, “Four-dimensional black holes in string theory,” *Phys. Rev. D* **48** (1993) 5784–5797, [arXiv:hep-th/9305083](#).
- [41] S. J. Gates, Jr. and T. Hübsch, “Unidexterous locally supersymmetric actions for Calabi–Yau compactifications,” *Phys. Lett.* **B226** (1989) 100.
- [42] S. J. Gates, Jr. and T. Hübsch, “Calabi–Yau heterotic strings and unidexterous sigma models,” *Nucl. Phys.* **B343** (1990) 741–774.

- [43] B. R. Greene and M. R. Plesser, “Duality in Calabi–Yau moduli space,” *Nucl. Phys.* **B338** (1990) 15–37.
- [44] P. Berglund and T. Hübsch, “A generalized construction of mirror manifolds,” *Nucl. Phys.* **B393** no. 1-2, (1993) 377–391, [arXiv:hep-th/9201014 \[hep-th\]](#). [AMS/IP Stud. Adv. Math. 9 (1998) 327].
- [45] P. Berglund and M. Henningson, “Landau–Ginzburg orbifolds, mirror symmetry and the elliptic genus,” *Nucl. Phys.* **B433** (1995) 311–332, [arXiv:hep-th/9401029 \[hep-th\]](#).
- [46] M. Krawitz, *FJRW rings and Landau–Ginzburg Mirror Symmetry*. PhD thesis, University of Michigan, Ann Arbor, MI, 2010. [arXiv:0906.0796 \[math.AG\]](#).
- [47] S. Cecotti, L. Girardello, and A. Pasquinucci, “Nonperturbative aspects and exact results for the  $N = 2$  Landau–Ginsburg models,” *Nucl. Phys.* **B328** no. 3, (1989) 701–722.
- [48] V. V. Batyrev, “Dual polyhedra and mirror symmetry for Calabi–Yau hypersurfaces in toric varieties,” *J. Alg. Geom.* **3** no. 3, (1994) 493–535, [arXiv:alg-geom/9310003](#).
- [49] L. A. Borisov, “Berglund–Hübsch mirror symmetry via vertex algebras,” *Comm. Math. Phys.* **320** no. 1, (2013) 73–99, [arXiv:1007.2633 \[math.AG\]](#).
- [50] V. V. Batyrev and L. A. Borisov, “Dual cones and mirror symmetry for generalized Calabi–Yau manifolds,” in *Mirror symmetry, II*, vol. 1 of *AMS/IP Stud. Adv. Math.*, pp. 71–86. Amer. Math. Soc., Providence, RI, 1997. [arXiv:math/9402002 \[math.AG\]](#).
- [51] M. Kontsevich, “Homological algebra of mirror symmetry,” in *International Congress of Mathematicians*, S. D. Chatterji, ed., pp. 120–139. Birkhäuser Basel, Basel, 1995. [arXiv:alg-geom/9411018 \[alg-geom\]](#).
- [52] M. Kontsevich, “Mirror symmetry in dimension 3,” *Séminaire Bourbaki (1994–95) exp. n° 801 in Astérisque* **237** (1996) 275–293. <http://eudml.org/doc/110202>.
- [53] M. Gross and B. Siebert, “Intrinsic mirror symmetry and punctured Gromov–Witten invariants,” [arXiv:1609.00624 \[math.AG\]](#).
- [54] P. Berglund and T. Hübsch, “On Calabi–Yau generalized complete intersections from Hirzebruch varieties and novel K3-fibrations,” *Adv. Theor. Math. Phys.* **22** no. 2, (2018) 261 – 303, [arXiv:1606.07420 \[hep-th\]](#).
- [55] P. Berglund and T. Hübsch, “A generalized construction of Calabi–Yau models and mirror symmetry,” *SciPost* **4** no. 2, (2018) 009 (1–30), [arXiv:1611.10300 \[hep-th\]](#).
- [56] P. Berglund and T. Hübsch, “Hirzebruch surfaces, Tyurin degenerations and toric mirrors: Bridging generalized Calabi–Yau constructions,” *Adv. Theor. Math. Phys.* **26** no. 8, (2022) 2541–2598, [arXiv:2205.12827 \[hep-th\]](#).
- [57] P. Berglund and T. Hübsch, “Chern characteristics and Todd–Hirzebruch identities for transpolar pairs of toric spaces,” [arXiv:2403.07139 \[hep-th\]](#).
- [58] T. Hübsch, “Ricci–flat mirror hypersurfaces in spaces of general type,” in *Proceedings of the 11th Mathematical Physics Meeting (Sep. 2–6. 2024)*, B. Dragovich, ed. 2025. [arXiv:2501.11684 \[hep-th\]](#).
- [59] T. Hübsch, “Beyond algebraic superstring compactification,” *Axioms* **14** no. 4, (2, 2025) 236, [arXiv:2502.08002 \[hep-th\]](#).
- [60] K. Schwarzschild, “On the gravitational field of a mass point according to Einstein’s theory,” *Sitzungsber. Preuss. Akad. Wiss. Berlin (Math. Phys.)* **1916** (1916) 189–196, [arXiv:physics/9905030](#). Original title: “Über das Gravitationsfeld eines Massenpunktes nach der Einsteinschen Theorie”.
- [61] E. Kasner, “Finite representation of the solar gravitational field in flat space of six dimensions,” *American Journal of Mathematics* **43** no. 2, (1921) 130–133. <http://www.jstor.org/stable/2370246>.
- [62] A. Einstein and N. Rosen, “The particle problem in the general theory of relativity,” *Phys. Rev.* **48** (Jul, 1935) 73–77.
- [63] C. Fronsdal, “Completion and embedding of the Schwarzschild solution,” *Phys. Rev.* **116** no. 3, (Nov, 1959) 778–781.
- [64] M. Masuda, “Unitary toric manifolds, multi-fans and equivariant index,” *Tohoku Math. J. (2)* **51** no. 2, (1999) 237–265. <http://projecteuclid.org/euclid.ojm/1178224815>.
- [65] M. Masuda, “From convex polytopes to multi-polytopes,” *Notes Res. Inst. Math. Analysis* **1175** (2000) 1–15. <http://hdl.handle.net/2433/64488>.
- [66] A. Hattori and M. Masuda, “Theory of multi-fans,” *Osaka J. Math.* **40** (2003) 1–68, [arXiv:math/0106229 \[math.SG\]](#). <http://projecteuclid.org/euclid.ojm/1153493035>.
- [67] M. Masuda and T. Panov, “On the cohomology of torus manifolds,” *Osaka Journal of Mathematics* **43** no. 3, (2006) 711 – 746, [arXiv:math/0306100 \[math.AT\]](#).

- [68] A. Hattori and M. Masuda, “Elliptic genera, torus manifolds and multi-fans,” *Int. J. of Math.* **16** no. 9, (July, 2006) 957–998, [arXiv:math/0107014](#) [[math.SG](#)].
- [69] A. Hattori, “Elliptic genera, torus orbifolds and multi-fans; II,” *Int. J. Math* **17** no. 06, (2006) 707–735, [arXiv:math/0501392](#) [[math.AT](#)].
- [70] Y. Nishimura, “Multipolytopes and convex chains,” *Proc. Steklov Inst. Math.* **252** (2006) 212–224.
- [71] H. Ishida, “Invariant stably complex structures on topological toric manifolds,” *Osaka J. Math.* **50** (2013) 795–806.
- [72] M. W. Davis and T. Januszkiewicz, “Convex polytopes, Coxeter orbifolds and torus actions,” *Duke Math. J.* **62** no. 2, (1991) 417–451.
- [73] H. Ishida, Y. Fukukawa, and M. Masuda, “Topological toric manifolds,” *Moscow Math. J.* **13** no. 1, (2013) 57–98, [arXiv:1012.1786](#) [[math.AT](#)].
- [74] V. Buchstaber and T. Panov, *Toric Topology*. No. 204 in Mathematical Surveys and Monographs. American Mathematical Society, Providence, RI, 2015. [arXiv:1210.2368](#) [[math.AT](#)].
- [75] D. Jang, “Four dimensional almost complex torus manifolds,” [arXiv:2310.11024](#) [[math.DG](#)].
- [76] N. MacFadden and E. Sheridan, “Calabi-Yau Threefolds from Vex Triangulations,” [arXiv:2512.14817](#) [[hep-th](#)].
- [77] F. Hirzebruch, “Über eine Klasse von einfach-zusammenhängenden komplexen Mannigfaltigkeiten,” *Math. Ann.* **124** (1951) 77–86.
- [78] M. Kreck and D. Crowley, “Hirzebruch surfaces,” *Bulletin of the Manifold Atlas* no. 19-22, (2011) .
- [79] R. Brooks, F. Muhammad, and S. J. Gates, Jr., “Unidexterous  $D = 2$  supersymmetry in superspace,” *Nucl. Phys.* **B268** (1986) 599–620.
- [80] R. Brooks and S. J. Gates, Jr., “Unidexterous  $D = 2$  supersymmetry in superspace. 2. quantization,” *Phys. Lett.* **B184** (1987) 217.
- [81] R. Brooks, F. Muhammad, and S. J. Gates, Jr., “Matter coupled to  $D = 2$  simple unidexterous supergravity, local (supersymmetry)\*\*2 and strings,” *Class. Quant. Grav.* **3** (1986) 745–751.
- [82] S. J. Gates, Jr., R. Brooks, and F. Muhammad, “Unidexterous superspace: The flux of (super)strings,” *Phys. Lett.* **B194** (1987) 35.
- [83] T. Hübsch, “Haploid (2,2)-superfields in 2-dimensional space-time,” *Nucl. Phys.* **B555** no. 3, (1999) 567–628, [arXiv:hep-th/9901038](#).
- [84] R. Q. Almkahhal and T. Hübsch, “Gauging Yang–Mills symmetries in 1+1-dimensional space-time,” *Int. J. Mod. Phys. A* **16** no. 29, (2001) 4713–4768, [arXiv:hep-th/9910007](#).
- [85] T. Hübsch and I. E. Petrov, “Worldsheet matter superfields on half-shell,” *J. Phys. A* **43** (2010) 295206, [arXiv:0912.1038](#).
- [86] E. Braaten, T. L. Curtright, and C. K. Zachos, “Torsion and geometrostasis in nonlinear sigma models,” *Nucl. Phys.* **B260** (1985) 630. [Erratum: *Nucl. Phys.***B266** (1986) 748].
- [87] H. Eichenherr, “ $SU(N)$  invariant non-linear  $\sigma$  models,” *Nuclear Physics B* **146** no. 1, (1978) 215–223. Errata: *Nucl. Phys.***B146** (1978) 215.
- [88] T. Hübsch, “Chameleonic sigma-models,” *Phys. Lett.* **B247** (1990) 317–322.
- [89] T. Hübsch, “Of marginal kinetic terms and anomalies,” *Mod. Phys. Lett.* **A6** (1991) 1553–1559.
- [90] D. Bykov, “Sigma models as Gross–Neveu models,” *Teor. Mat. Fiz.* **208** no. 2, (2021) 165–179, [arXiv:2106.15598](#) [[hep-th](#)].
- [91] P. Berglund, G. Butbaia, T. Hübsch, V. Jejjala, D. Mayorga Peña, C. Mishra, and J. Tan, “Machine Learned Calabi–Yau Metrics and Curvature,” *Adv. Theor. Math. Phys.* **27** no. 4, (2023) 1107–1158, [arXiv:2211.09801](#) [[hep-th](#)].
- [92] E. Witten, “Quantum Field Theory, Grassmannians, and Algebraic Curves,” *Commun. Math. Phys.* **113** (1988) 529.
- [93] P. Berglund, S. H. Katz, and A. Klemm, “Mirror symmetry and the moduli space for generic hypersurfaces in toric varieties,” *Nucl. Phys.* **B456** (1995) 153–204, [arXiv:hep-th/9506091](#) [[hep-th](#)].
- [94] T. Oda and H. S. Park, “Linear Gale transforms and Gel’fand–Kapranov–Zelevinskij decompositions,” *Tôhoku Math. J.* **43** (1991) 375–399.
- [95] L. B. Anderson, F. Apruzzi, X. Gao, J. Gray, and S.-J. Lee, “A new construction of Calabi–Yau manifolds: Generalized CICYs,” *Nucl. Phys.* **B906** (2016) 441–496, [arXiv:1507.03235](#) [[hep-th](#)].

- [96] A. Garbagnati and B. van Geemen, “A remark on generalized complete intersections,” *Nucl. Phys.* **B925** (2017) 135–143, [arXiv:1708.00517 \[math.AG\]](#).
- [97] T. T. Wu and C. N. Yang, “Concept of nonintegrable phase factors and global formulation of gauge fields,” *Phys. Rev. D* **12** (1975) 3845–3857.
- [98] T. Hübsch, “Calabi–Yau manifolds — motivations and constructions,” *Commun. Math. Phys.* **108** (1987) 291–318.
- [99] P. S. Green and T. Hübsch, “Calabi–Yau manifolds as complete intersections in products of projective spaces,” *Comm. Math. Phys.* **109** (1987) 99–108.
- [100] P. Candelas, A. M. Dale, C. A. Lütken, and R. Schimmrigk, “Complete intersection Calabi–Yau manifolds,” *Nucl. Phys.* **B298** (1988) 493.
- [101] P. S. Green, T. Hübsch, and C. A. Lütken, “All the hodge numbers for all Calabi–Yau complete intersections,” *Class. Q. Grav.* **6** (1989) 105–124.
- [102] P. S. Green and T. Hübsch, “Calabi–Yau hypersurfaces in products of semi-ample surfaces,” *Comm. Math. Phys.* **115** (1988) 231–246.
- [103] T. Hübsch and S.-T. Yau, “An  $SL(2, \mathbb{C})$  action on chiral rings and the mirror map,” *Mod. Phys. Lett.* **A7** (1992) 3277–3289.
- [104] B. Dwork, “ $p$ -adic cycles,” *Inst. Hautes Études Sci. Publ. Math.* **37** (1969) 27–115.
- [105] P. Candelas, X. C. De la Ossa, P. S. Green, and L. Parkes, “An exactly soluble superconformal theory from a mirror pair of Calabi–Yau manifolds,” *Phys. Lett. B* **258** (1991) 118–126.
- [106] P. Candelas, X. C. De La Ossa, P. S. Green, and L. Parkes, “A pair of Calabi–Yau manifolds as an exactly soluble superconformal theory,” *Nucl. Phys. B* **359** (1991) 21–74.
- [107] P. Berglund, P. Candelas, X. d. l. Ossa, A. Font, T. Hübsch, D. Jancic, and F. Quevedo, “Periods for Calabi–Yau and Landau–Ginzburg vacua,” *Nucl. Phys.* **B419** (1994) 352–403, [arXiv:hep-th/9308005](#).
- [108] T. Hibi, “Star-shaped complexes and Ehrhart polynomials,” *Proc. Am. Math. Soc.* **123** no. 3, (1995) 723–726.
- [109] M. Gross, “The deformation space of Calabi–Yau  $n$ -folds with canonical singularities can be obstructed,” in *Mirror Symmetry II*, B. Greene and S.-T. Yau, eds., Studies in Advanced Mathematics, p. 1. AMS and Int. Press, Providence, RI and Cambridge, MA, 1997. [arXiv:alg-geom/9402014 \[alg-geom\]](#).
- [110] Y. Ruan, “Topological sigma model and Donaldson-type invariants in Gromov theory,” *Duke Mathematical Journal* **83** no. 2, (1996) 461 – 500.
- [111] Y.-C. Huang and W. Taylor, “Fibration structure in toric hypersurface Calabi–Yau threefolds,” [arXiv:1907.09482 \[hep-th\]](#).
- [112] P. Jefferson and M. Kim, “On the intermediate Jacobian of M5-branes,” [arXiv:2211.00210 \[hep-th\]](#).
- [113] A. Khovanskii and A. Pukhlikov, “Finitely additive measures of virtual polytopes,” *St. Petersburg Math. J.* **4** no. 2, (1993) 337–356. Transl. from *Algebra and Analysis*, **4** (2) (1992) 161–185.
- [114] A. Khovanskii and A. Pukhlikov, “A Riemann–Roch theorem for integrals and sums of quasipolynomials over virtual polytopes,” *St. Petersburg Math. J.* **4** no. 4, (1993) 789–812. Transl. from *Algebra and Analysis*, **4** (4) (1992) 188–216.
- [115] Y. Karshon and S. Tolman, “The moment map and line bundles over presymplectic toric manifolds,” *J. Diff. Geom.* **38** no. 3, (1993) 465–484. <https://projecteuclid.org/euclid.jdg/1214454478>.
- [116] H. Fan, T. Jarvis, and Y. Ruan, “The Witten equation, mirror symmetry and quantum singularity theory,” *Annals of Mathematics* **178** (2013) 1–106, [arXiv:0712.4021 \[math.AG\]](#). <http://www.jstor.org/stable/23470821>.
- [117] M. Krawitz, N. Priddis, P. Acosta, N. Bergin, and H. Rathnakumara, “FJRW-rings and mirror symmetry,” *Comm. Math. Phys.* **296** no. 1, (Oct., 2009) 145–174, [arXiv:0903.3220 \[math.AG\]](#).
- [118] M. Krawitz, *FJRW rings and Landau–Ginzburg Mirror Symmetry*. PhD thesis, University of Michigan, Ann Arbor, MI, 2010. [arXiv:0906.0796 \[math.AG\]](#).
- [119] W. Ebeling and A. Takahashi, “Mirror symmetry between orbifold curves and cusp singularities with group action,” *Int. Math. Res. Not.* **2013** no. 10, (April, 2012) 2240–2270, [arXiv:1103.5367 \[math.AG\]](#).
- [120] M. Artebani, P. Comparin, and R. Guilbot, “Families of Calabi–Yau hypersurfaces in  $\mathbb{Q}$ -Fano toric varieties,” *J. Math. Pure & Appl.* **106** no. 2, (2016) 319–341, [arXiv:1501.05681 \[math.AG\]](#).
- [121] P. S. Aspinwall and M. R. Plesser, “General mirror pairs for gauged linear sigma models,” *JHEP* **1511** (2015) 029, [arXiv:1507.00301 \[hep-th\]](#).

- [122] D. Favero and T. L. Kelly, “Derived categories of BHK mirrors,” *Adv. Math.* **352** (2019) 943–980, [arXiv:1602.05876 \[math.AG\]](#).
- [123] S. Parkhomenko, “Spectral flow construction of mirror pairs of CY orbifolds,” *Nucl. Phys. B* **985** (2022) 116005, [arXiv:2208.11612 \[hep-th\]](#).
- [124] A. Belavin and S. Parkhomenko, “Mirror symmetry and new approach to constructing orbifolds of Gepner models,” [arXiv:2311.15403 \[hep-th\]](#).
- [125] S. Parkhomenko, “Conformal bootstrap and Mirror symmetry of states in Gepner models,” [arXiv:2407.07555 \[hep-th\]](#).
- [126] C.-H. Cho, D. Choa, and W. Jeong, “Berglund-Hübsch mirrors of invertible curve singularities via Floer theory,” [arXiv:2410.14678 \[math.SG\]](#). <https://arxiv.org/abs/2410.14678>.
- [127] M. Masuda and S. Park, “Toric origami manifolds and multi-fans,” *Proc. Steklov Inst. Math.* **286** (May, 2014) 308–323, [arXiv:1305.6347 \[math.SG\]](#).
- [128] P. Berglund and M. Lathwood, “Tropical periods for Calabi–Yau hypersurfaces in non-Fano toric varieties,” [arXiv:2212.11906 \[hep-th\]](#).
- [129] V. Buchstaber and N. Ray, “Tangential structures on toric manifolds and connected sums of polytopes,” *Internat. Math. Res. Notices* **4** (2001) 193–219, [arXiv:math/0010025 \[math.AT\]](#).
- [130] Y. Cui and A. Gholampour, “Equivariant vector bundles over topological toric manifolds,” [arXiv:2504.12467 \[math.DG\]](#). <https://arxiv.org/abs/2504.12467>.
- [131] Y. Cui, “Klyachko vector bundles over topological toric manifolds,” [arXiv:2504.02205 \[math.AG\]](#). <https://arxiv.org/abs/2504.02205>.